ECMWF

European Centre for Medium-Range Weather Forecasts

Newsletter

No. 164 | Summer 2020

Publication policy

The ECMWF Newsletter is published quarterly. Its purpose is to make users of ECMWF products, collaborators with ECMWF and the wider meteorological community aware of new developments at ECMWF and the use that can be made of ECMWF products. Most articles are prepared by staff at ECMWF, but articles are also welcome from people working elsewhere, especially those from Member States and Co-operating States. The ECMWF Newsletter is not peer-reviewed.

Any queries about the content or distribution of the ECMWF Newsletter should be sent to Georg.Lentze@ecmwf.int

Guidance about submitting an article is available at *www.ecmwf.int/en/about/media-centre/media-resources*

Meeting the challenge

The last few months have been challenging in some respects but exciting in many others. Challenging because, like other organisations, ECMWF continues to be affected by the COVID-19 pandemic. Most of our staff still work from home, and all recent training courses, workshops and seminars have been held remotely. There is also a continuing impact on the availability of some of the Earth system observations used in numerical weather prediction. But recent months have also been exciting because of the way we have managed to turn some of those challenges into opportunities and to continue to advance weather science as well as operational forecasting.

Examples of exciting pieces of work presented in this Newsletter include implementing a wide-ranging upgrade of our Integrated Forecasting System to IFS Cycle 47r1; fine-tuning a major moist physics upgrade that has been in the making for the last five years; helping the Croatian Meteorological and Hydrological Service (DHMZ) to back up its production after an earthquake; adding new observations to alleviate the impact of losing others because of COVID-19; developing environmental monitoring tools to facilitate research on the spread of COVID-19; and successfully delivering virtual training events, workshop and seminars.

An aspect that shines through in these achievements is the close collaboration between the broad range of experts we have at ECMWF and between the Centre and external partners. One of the improvements brought by IFS Cycle 47r1 is a sharp reduction in large-scale biases of ECMWF analyses and forecasts in the stratosphere. Identifying and addressing the root cause of these biases is the fruit of close collaboration between experts in atmospheric physics and numerical methods at the Centre and beyond. Meanwhile, the moist physics upgrade was partly motivated by the plan to dramatically increase the resolution of our global ensemble forecasts. This change requires coordinated work on all aspects of the IFS: computing, data assimilation and Earth system modelling. The moist physics work, to be implemented in IFS Cycle 48r1, is an example of bringing such joined-up work to a successful conclusion.

On the COVID-19 front, the EU-funded Copernicus Atmosphere Monitoring Service (CAMS) and Copernicus Climate Change Service (C3S) implemented by ECMWF have worked together, in consultation with the European Commission, to develop tools that will help researchers and policymakers to understand possible links between COVID-19, climate and atmospheric composition. And the loss of observations has been alleviated by rapidly working with partners to enable the assimilation of new observations.

Finally, collaboration between forecasters and computing specialists made it possible to back up DHMZ's production at ECMWF, and ECMWF's event organisers and technicians worked together to continue to deliver training courses, workshops and seminars that make the most of the virtual format. In these challenging times, I would like to address my sincere thanks to all staff at ECMWF and to all our partners.

Florence Rabier
Director-General

Contents

Editor Georg Lentze • **Typesetting & Graphics** Anabel Bowen • **Cover** Photo: mm88 / iStock / Getty Images Plus

Warm intrusions into the Arctic in April 2020

Linus Magnusson, Jonathan Day, Irina Sandu (all ECMWF), Gunilla Svensson (Stockholm University)

Warm spells in the central Arctic during winter and spring are typically associated with intrusions of warm and moist air from the mid-latitudes (warm air intrusions hereafter). Two such events took place in April 2020. They passed the German icebreaker Polarstern, which was drifting in sea ice as part of the Multidisciplinary drifting Observatory for the Study of Arctic Climate (MOSAiC) campaign. In both cases, the surface temperature measured on Polarstern rose from the normal April temperature of around –20°C to around 0°C. ECMWF forecasts supported targeted observations made during this period, which will in turn help the Centre to improve its ability to predict warm air intrusions.

MOSAiC is a one-year observational campaign linked to the World Meteorological Organization's Year of Polar Prediction (YOPP) project. YOPP aims to understand atmospheric, ocean and sea-ice processes and advance prediction capabilities in polar regions. The MOSAiC campaign started in October 2019. YOPP and MOSAiC are led by the Alfred Wegener Institute (AWI, Germany), and the US National Oceanic and Atmospheric Administration (NOAA) coordinates forecast evaluation at MOSAiC.

Targeted observations

The third period of enhanced Arctic observations during YOPP took place in spring 2020 to complement the MOSAiC campaign. It took the form of a targeted observing period (TOP), which was different from the earlier special observing periods (SOPs) in 2018. In the TOPs, extra observations were only requested during selected meteorological situations of relevance for the Arctic. During this TOP, additional radiosondes were launched from different stations situated along warm air intrusions in order to shed light on the processes governing these situations. During the period of the warm air events, when Polarstern was located north of Svalbard, four radiosondes a day were launched at several upstream locations and seven a day on board Polarstern.

Although the two warm air intrusion events on 16 and 19 April were close in time, they were associated with different synoptic patterns. In the first event, the warm air was pushed to the northeast in front of a trough over Scandinavia, while in the second event the warm air was transported over the Atlantic on the western side of a ridge that developed over Scandinavia. The second case is a more typical flow configuration for creating warm conditions in the Atlantic sector of the Arctic.

Valuable guidance

Various ECMWF forecast products were used in the planning for the TOP, such as the Extreme Forecast Index (EFI) for temperature and water-vapour flux, upper-level flow forecasts and meteograms for the Polarstern location. Evaluating the performance of all forecasts for 2-metre maximum temperature valid on 19 April, the ensemble had a clear signal 7–8 days in advance about warmer than normal conditions at the location of Polarstern. The EFI product for 2-metre maximum temperature from five days before 19 April also flagged up the risk of unusually high temperatures.
By 19 April, the first warm air intrusion was being advected to the east (north of Russia) and the second one was north of Svalbard, as predicted. The second event was associated with large uncertainties due to the narrow nature of the warm-air feature. For example, in the forecast from 15 April, while most of the members indicated a very high daily maximum temperature, many ensemble members ended the warm spell too early at the Polarstern location, resulting in massive temperature errors during most parts of the day. Although there were large uncertainties in the timing and details of the event, the ECMWF forecasts gave valuable guidance for observation campaign planning.

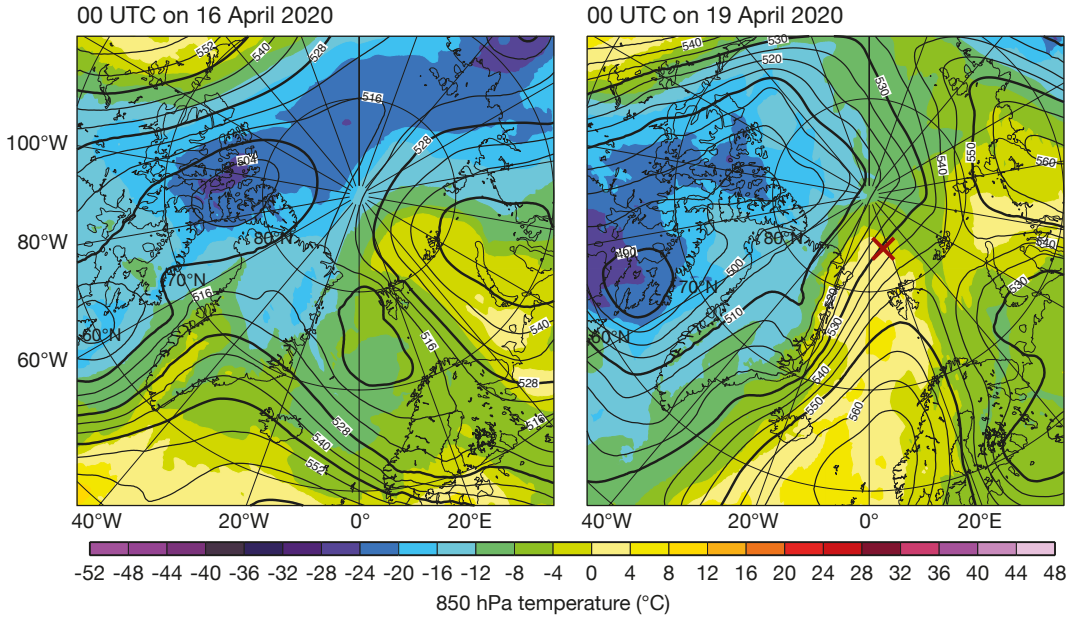

Synoptic situation on 16 and 19 April. Analysis of geopotential height at 500 hPa (contours) and temperature at 850 hPa (shading) for 00 UTC on 16 April 2020 (left) and 00 UTC on 19 April (right). The cross shows the approximate location of Polarstern on 19 April.

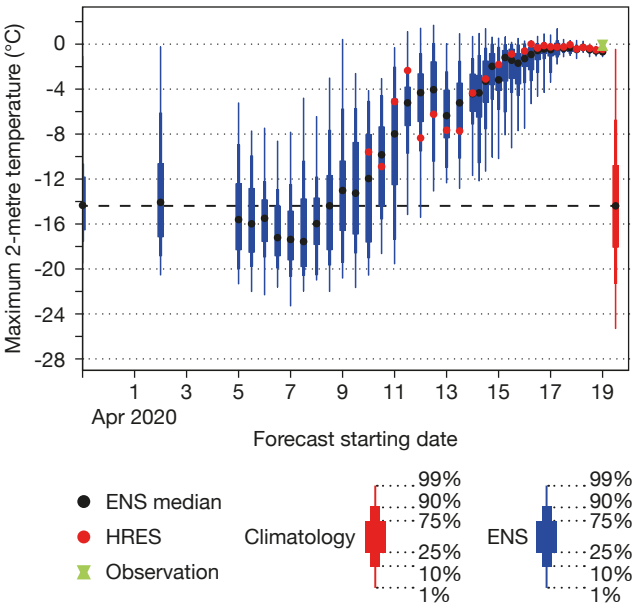

Evolution of forecasts for the 19 April warm air intrusion. The plot shows ensemble forecasts with different starting times for maximum 2-metre temperature for the Polarstern location on 19 April.

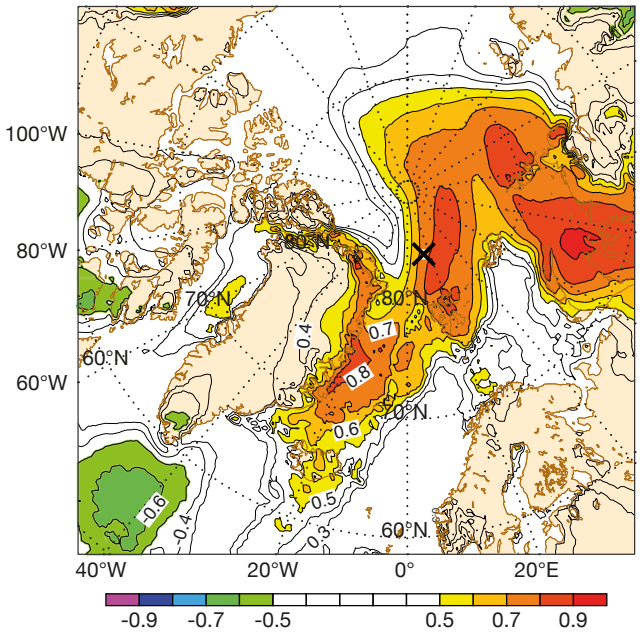

Two-metre maximum temperature EFI. The chart shows the 5-day forecast from 00 UTC on 15 April 2020 of the EFI for 2-metre maximum temperature on 19 April.

Outlook

The data collected during the MOSAiC campaign and the YOPP special observing periods will be used for model evaluation and development at ECMWF. To correctly forecast warm air intrusions and associated impacts, several aspects such as the origin and nature of the air mass, synoptic conditions, interactions with sea ice and mixed-phase cloud processes need to be correctly captured. It is therefore necessary to understand the physical mechanisms governing such events in order to improve the forecasting system. To this end, observations such as the ones from MOSAiC and YOPP are essential.

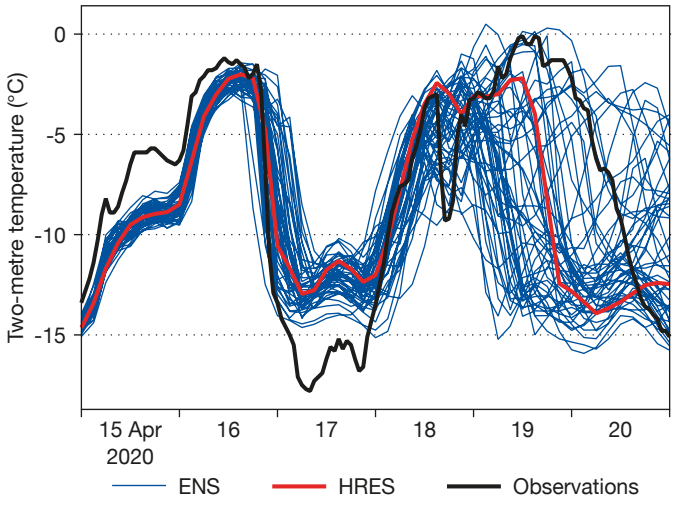

Predictions and Polarstern observations. Point forecast from 15 April 00 UTC for the location of Polarstern on 19 April for 2-metre temperature from the high-resolution forecast (HRES), the ensemble forecast (ENS) and observations from Polarstern.

New observations since April 2020

The following new observations have been activated in the operational ECMWF assimilation system since April 2020.

Observations	Main impact	Activation date
AFIRS aircraft data	Temperature and wind	12 May 2020
Radiances from MWRI on FY-3D	Total column water vapour, clouds, dynamics	13 May 2020
Atmospheric Motion Vectors from NOAA-20 VIIRS	Tropospheric Wind	13 May 2020
Radiosonde descent data over Germany	Wind, temperature and humidity	17 June 2020
Radio occultation bending angles from SPIRE satellites	Temperature and winds in upper troposphere/lower stratosphere	13 May 2020
TAMDAR aircraft data	Temperature and wind	17 June 2020

Statistical post-processing of ECMWF forecasts at the Belgian met service

Stéphane Vannitsem, Jonathan Demaeyer (both Royal Meteorological Institute of Belgium & EUMETNET)

The Royal Meteorological Institute (RMI) of Belgium has recently implemented a post-processing system for ECMWF's medium-range ensemble forecasts. First tests show that the system performs well.

Motivation

Statistical post-processing techniques have been used since the sixties to partly correct forecasting errors or to predict observables not represented in models. The first attempts used linear regression to model the relationship between past forecasts and observations. The results were then used to adjust new forecasts. Since then, many other techniques have been developed, in particular for ensemble forecasts. Such techniques have been shown to be necessary to optimise weather forecasts whatever the quality of the model. That is why RMI has been working on a technique that can be applied to ECMWF medium-range ensemble forecasts.

Implementation

In statistical post-processing, statistics are calculated to determine the relationship between forecasts and observations. This means that a set of past forecasts and observations have to be available for an appropriate correction scheme to be developed. As models are often upgraded by changing the model physics or dynamics, the biases present in successive model versions are likely to change. This can degrade the quality of the statistical correction scheme. To avoid such a degradation, ECMWF produces re-forecasts based on the latest model version and on initial conditions supplied by a suitable reanalysis.

At RMI, as in most operational weather forecasting centres, statistical post-processing is recognised as a priority for future development of the forecasting suite. A sophisticated linear post-processing scheme for ensemble forecasts, known as the Member-by-Member approach (MBM), has been implemented for ECMWF ensemble forecasts, taking advantage of the re-forecasts produced by the Centre. The system generates adjusted ensemble forecasts for 2-metre temperature, maximum and minimum temperature, and wind gusts at 11 weather stations in Belgium. Those are reference stations of 11 coherent climatological regions covering Belgium. Pre-operational and operational implementation started in mid-February 2020 and mid-June 2020, respectively.

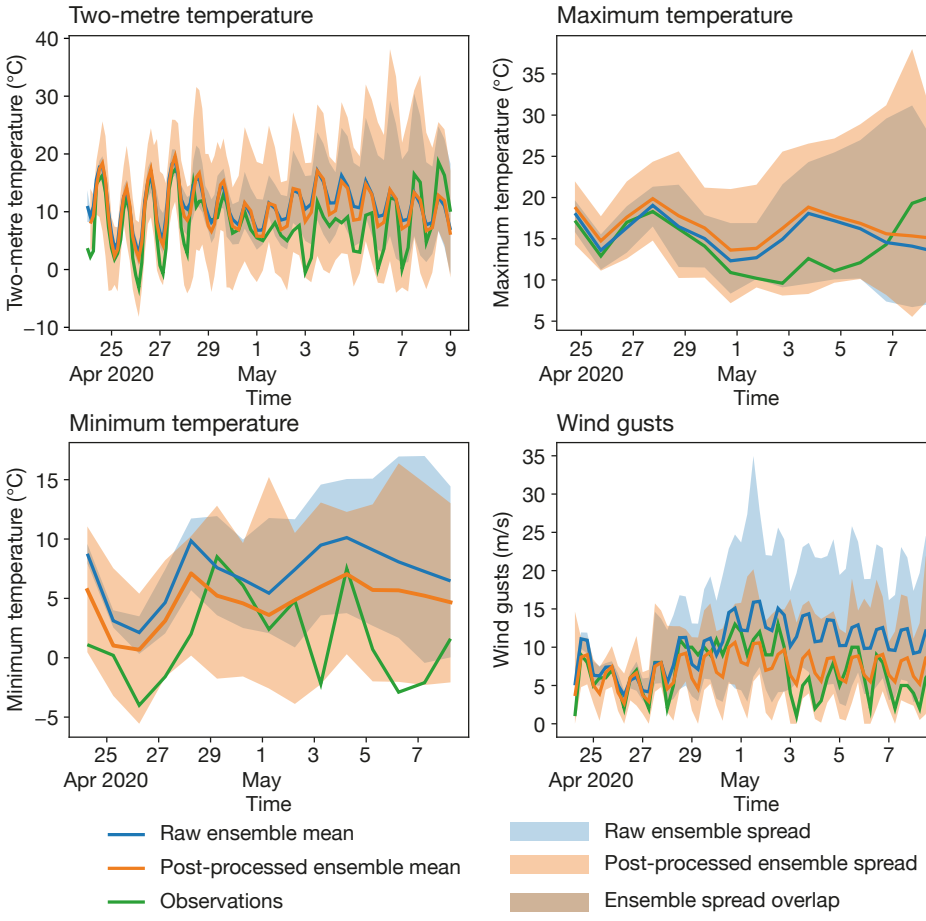

Observations and raw/ post-processed forecasts. The plots show observations and the spread (minimum to maximum values) and the mean of raw and post-processed ensemble forecasts starting from 24 April 2020 at the Elsenborn weather station for 2-metre temperature, maximum 2-metre temperature, minimum 2-metre temperature and wind gusts.

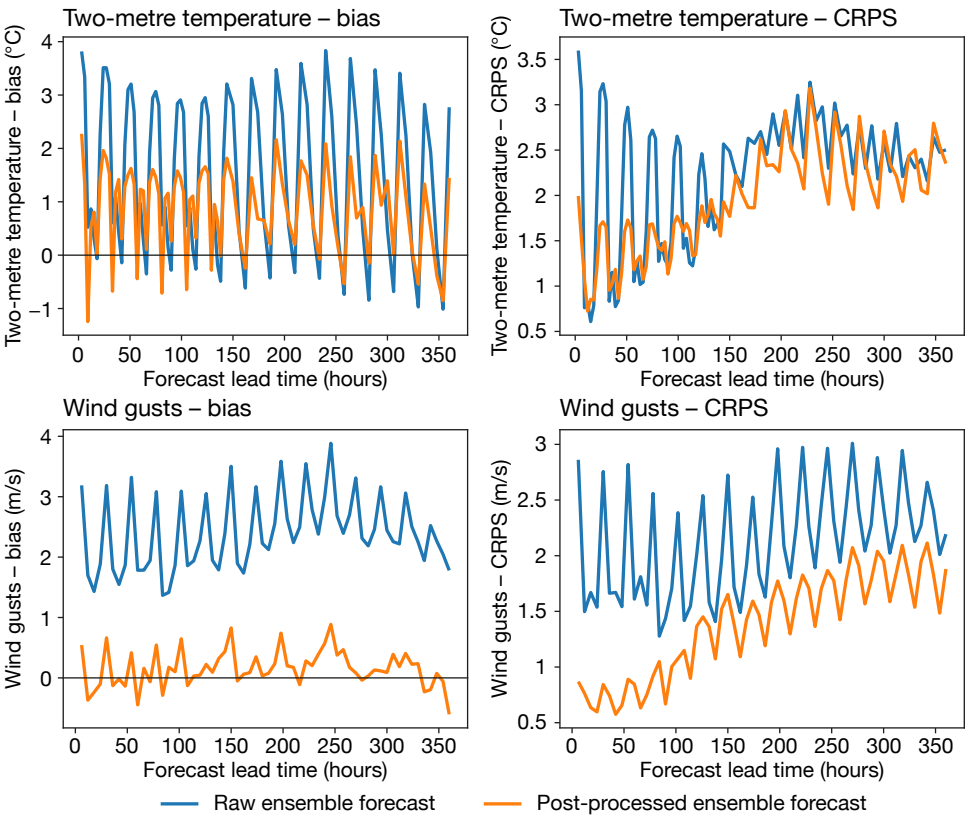

Forecast skill comparison. The plots show forecast skill for raw and post-processed ensemble forecasts for April 2020 as verified by in-situ observations at the Elsenborn weather station in terms of 2-metre temperature forecast ensemble mean bias, 2-metre temperature forecast CRPS, wind gust forecast ensemble mean bias and wind gust forecast CRPS. Smaller CRPS values indicate better forecasts.

Technically, the system is implemented within a Docker app written in Python and maintained using Anaconda. These modern tools enable an easy transfer from research to operations. The core of the app is a new Python post-processing module implementing various MBM approaches, which can easily be re-used for other projects. The output of the correction scheme for the ensemble forecast at 00 UTC is provided to the forecasters of the RMI weather office in parallel with the raw forecasts. This is done by filing a preliminary meteorological report, which can still be modified by the forecasters. The post-processed output will also soon be available in RMI's INDRA information system.

Results

A typical ensemble forecast produced by the scheme is shown in the first figure for the Elsenborn weather station located in eastern Belgium. For most variables, the forecast is improved, in particular the wind gust forecast, which is considerably shifted to smaller values closer to observations.

Figure 2 shows two scores for two of the variables. Biases are shown in the left-hand panels and the continuous ranked probability score (CRPS) in the right-hand panels, for the month of April 2020 for Elsenborn. The biases are reduced for both variables and the CRPS scores show a good improvement.

The statistical post-processing scheme is already delivering large corrections, and new developments are expected to add other variables and to implement the scheme on a grid. In a future Newsletter article, a detailed evaluation of the scheme will be presented together with upcoming operational developments.

Croatian met service backs up its production at ECMWF after earthquake

Xavier Abellan (ECMWF), Kristian Horvath, Izidor Pelajić, Antonio Stanešić (all DHMZ)

The Croatian Meteorological and Hydrological Service (DHMZ) has successfully backed up its operational production and essential services on ECMWF's High-Performance Computing Facility (HPCF) and the European Weather Cloud, following an earthquake that severely damaged DHMZ's headquarters in March this year. Despite the emergency situation, and without previous preparation, the backup system was put together in just a matter of days. The success of this project was made possible thanks to a joint effort by a number of staff from DHMZ together with many others at ECMWF, EUMETSAT and the weather software company IBL.

The IT infrastructure at DHMZ survived the earthquake, but it was clear that an alternative arrangement was

Earthquake damage inside. The earthquake damaged office areas in the DHMZ building.

required to ensure continuity of service, using off-site resources. In the days after the earthquake, stable communication channels were quickly established among key people at DHMZ, ECMWF and EUMETSAT to discuss the best migration strategy and possible options, and a plan to move forward was outlined.

It was agreed that numerical weather prediction (NWP) and some post-processing activities would be ported to ECMWF's HPCF, while some other essential services not fit for such infrastructure would use the European Weather Cloud. Within a week, the main components of the NWP system were running on the Centre's supercomputers, and the European Weather Cloud was hosting a number of other services. ECMWF dissemination streams and EUMETCast feeds were also configured to be delivered to the newly created locations. "I am hugely impressed by the prompt, effective response and support by ECMWF and EUMETSAT to DHMZ after the earthquake," says Dr Branka Ivančan-Picek, Director General of DHMZ.

Moving onto ECMWF's HPCF

DHMZ's NWP group maintains and develops the operational limited-area model ALADIN and its local applications. The model and the post-processing chain are hosted on DHMZ HPC and servers located in the DHMZ headquarters. After the earthquake, it was decided to establish a backup of NWP operations at ECMWF. A list of priority users was drawn up. The goal was to provide a backup solution to them and then to gradually include others. Until then DHMZ had had very little experience with ECMWF's HPCF: it had built only one version of the ALADIN model and one script for running the model integration.

As the local configuration was reviewed, it was clear that data assimilation would be too hard to set up in such a short time. The solution was to use the initial conditions obtained from an unperturbed member of A-LAEF (RC-LACE ensemble system), which was already running at ECMWF. For lateral boundary conditions (LBC), ECMWF products are used. In coordination with ECMWF, a new channel for LBC distribution was promptly established, so the same products distributed regularly to DHMZ were also sent directly to ECMWF's HPCF to feed into the ALADIN model. After this, hard work on the porting of different model configurations and post-processing started. With the help of ECMWF user documentation and guidance, in a little more than a week DHMZ had the first prototype of its operations backup running at ECMWF.

Days after the model was configured and had started to run, parallelised post-processing using conda environments and a python/bash framework was set up. It was essential to keep DHMZ's users informed about what was happening on a daily basis and what DHMZ was doing to mitigate the risk of failing to deliver its numerical products. End users were informed about the availability of products based on the operational backup at HPCF, which were ready to use in case of a major failure of DHMZ's local IT infrastructure and during occasional delays with local operations. DHMZ received a lot of appreciation for the work done from its critical end users, who felt safe knowing that they would not have any issues with their weather-related decision-making.

Getting on board the European Weather Cloud

All the IT infrastructure used to serve and display products to end users is also located in the damaged DHMZ headquarters. However, for those services the HPCF would not have been a feasible alternative. It was therefore proposed to back them up on the European Weather Cloud. After the project was created on the cloud, DHMZ managed to quickly provision an Ubuntu virtual machine (VM) with predefined options. All relevant components for a web server, such as Apache and PHP, were soon installed and configured. DHMZ found the documentation for creating a virtual machine clear and helpful, but to configure it some prior knowledge of system administration was required.

To ensure continuity of the remaining essential services, an attempt was made to recreate the forecasters' operational environment in the cloud. As DHMZ uses IBL's Visual Weather workstation, this was done in coordination with IBL as well as EUMETSAT, who provided both data and additional IT support through various channels. The operational environment in general consists of inputs, the core production part and a number of outputs. To facilitate this, three additional virtual machines (VMs) were set up.

A first reception VM was created, where a subset of EUMETCast (MSG and DWDSAT satellite data) is delivered by FTP (at first as a push service from EUMETCast Terrestrial). A second CentOS VM was dedicated to a VisualWeather visualisation and forecast production system, and a third VM was provisioned as a Network File System shared storage service for internal data manipulation. ECMWF model outputs were made available within the European Weather Cloud Object Storage service, ALADIN (HPCF version) data were imported directly, ICON data from the German national meteorological service (DWD) were collected over DWD's open data server, and US Global Forecast System data were also ingested into the system. With Global Telecommunication System data available over DWDSAT, LINET lightning data and MSG SEVIRI HRIT satellite data, most of the essential data are now available in the cloud system.

Visualisation and report production configuration were then transferred from DHMZ's native VisualWeather system to the newly created cloud instance. Forecasters now have access to a familiar system from their home

computers with relatively simple means through SSH and VNC services. DHMZ found that setting up the dissemination part proved to be the most challenging aspect, mostly due to a lack of understanding of the security features on ECMWF's side of the European Weather Cloud.

Future plans

The 5.3 magnitude earthquake on Sunday, 22 March 2020 and more than 30 aftershocks caused considerable damage to the 19th-century building hosting DHMZ in Zagreb. No one was injured during the event, but the building was deemed unsafe to work in. Staff managed to carry on with their duties remotely and to deliver the service to the public, relevant authorities and critical end users.

The operational production risk mitigation plan for the near future is to keep the backup of NWP and post-processing production on ECMWF's HPCF active until DHMZ acquires and puts into operations a new supercomputer, as well as ensuring that related essential services can be run on the European Weather Cloud.

The earthquake in Croatia was a reminder of how natural hazards can endanger the role of national meteorological services to serve society and protect lives and property. Through effective collaboration with ECMWF and EUMETSAT, DHMZ was able to ensure the resilience of its critical weather services in the time after the earthquake, while showcasing the usefulness of the European Weather Cloud and other services at ECMWF.

Many people were involved in making a success of this project. Beyond the authors, several other DHMZ experts should be acknowledged since they were instrumental in either setting up the backup (M. Hrastinski, E. Keresturi, S. Panežić) or establishing communication links (B. Matjačić, M. Tudor). A number of staff across departments at ECMWF and EUMETSAT, as well as IBL, also played a key role in ensuring a quick and smooth journey.

Earthquake damage outside. Some of the outside of the DHMZ building was also damaged.

New HPC Test and Early Migration System

Cristian Simarro

After ECMWF signed a four-year contract with Atos for the supply of its BullSequana XH2000 supercomputer, Atos started the installation of a high-performance computing (HPC) Test and Early Migration System (TEMS) at ECMWF's data centre in Reading, UK, in February 2020. The system comprises 60 nodes:

- 40 compute nodes (parallel jobs)
- 20 GPIL nodes (general purpose and interactive login).

The GPIL nodes are intended to integrate the interactive and post-processing work that is currently done on ecgate and the Linux Clusters.

One of the main differences between ECMWF's current Cray XC40 system and the future BullSequana XH2000 is the processor technology, which changes from Intel Broadwell to AMD EPYC Rome. Even though both implement variants of the ubiquitous x86_64 instruction set, the latter has many more processors. The new layout implies that a correct process binding configuration is fundamental to achieve good performance.

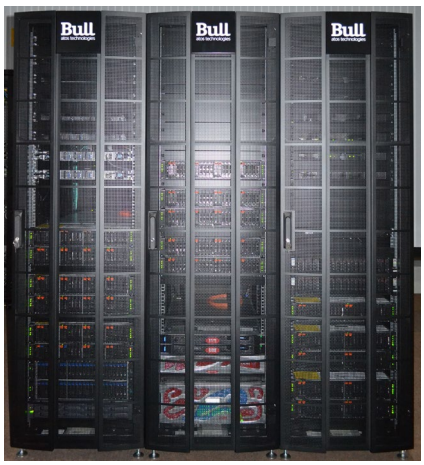

Test system. The HPC Test and Early Migration System supplied by Atos was installed at ECMWF in February 2020.

In addition, the queuing system will move from Cray's usage of aprun under the Portable Batch System (PBS) to Slurm/srun.

After the initial integration of the TEMS into the Centre's systems, ECMWF installed the environment 'module' system and other third-party software packages commonly required. Soon after, several teams across the organisation started to explore which different combinations of compilers and Message Passing Interface (MPI) implementations work best for different scenarios. First tests indicated that often best results appear to be achieved with a combination of the Intel compiler with Intel MPI or HPC-X-boosted OpenMPI for code development. Alternatively, the GNU compiler suite is available.

Since the computational capacity of the TEMS is small, and its configuration is ongoing, access is limited to ECMWF application migration teams and selected Member State users by invitation only (e.g. developers of Time-Critical suites).

The TEMS specification

60 nodes with:

- 2 x AMD Rome 7H12
- 512 GiB memory
- 1 TB local SSD (only in the GPIL nodes)

Copernicus contributes to coronavirus research

Vincent-Henri Peuch, Carlo Buontempo, Richard Engelen

Amid the coronavirus pandemic, there is widespread interest in up-to-date information about how the resulting lockdown is affecting air quality, but also how the climate and atmospheric composition might impact the spread of the virus. The Copernicus Climate Change Service (C3S) and Copernicus Atmosphere Monitoring Service (CAMS) – both implemented by ECMWF on behalf of the European Commission – are helping researchers, policymakers and citizens alike with quality-assured data and tools.

CAMS and COVID

CAMS is focusing on the relationship between exposure to air pollution and the development of the COVID-19 disease in populations exposed to the coronavirus, as well as the effects of lockdown measures on air quality.

A dedicated web-based CAMS COVID resource has provided information on air quality since March, and CAMS scientists are now investigating the connection between these air quality data and COVID-19. Maps of nitrogen dioxide, particulate matter and ozone – all known to be harmful to human health and to lower people's immune response, making them more vulnerable to viral attacks – are released daily. Time series show changes in the levels of pollutants, and animations help to visualise air pollution. The CAMS COVID resource was developed in response to significant interest in CAMS data after the pandemic began. The aim was to make the data easily accessible to businesses, policymakers and the wider public.

These data can, for instance, be used to explore the effects of lockdown measures on air quality. In February, CAMS observed a decrease in fine particulate matter over China's Hubei province compared to the same month in the previous three years. In mid-March, the CAMS analysis of atmospheric composition – produced by combining observations with models – showed that levels of nitrogen dioxide over northern Italy had been steadily decreasing since

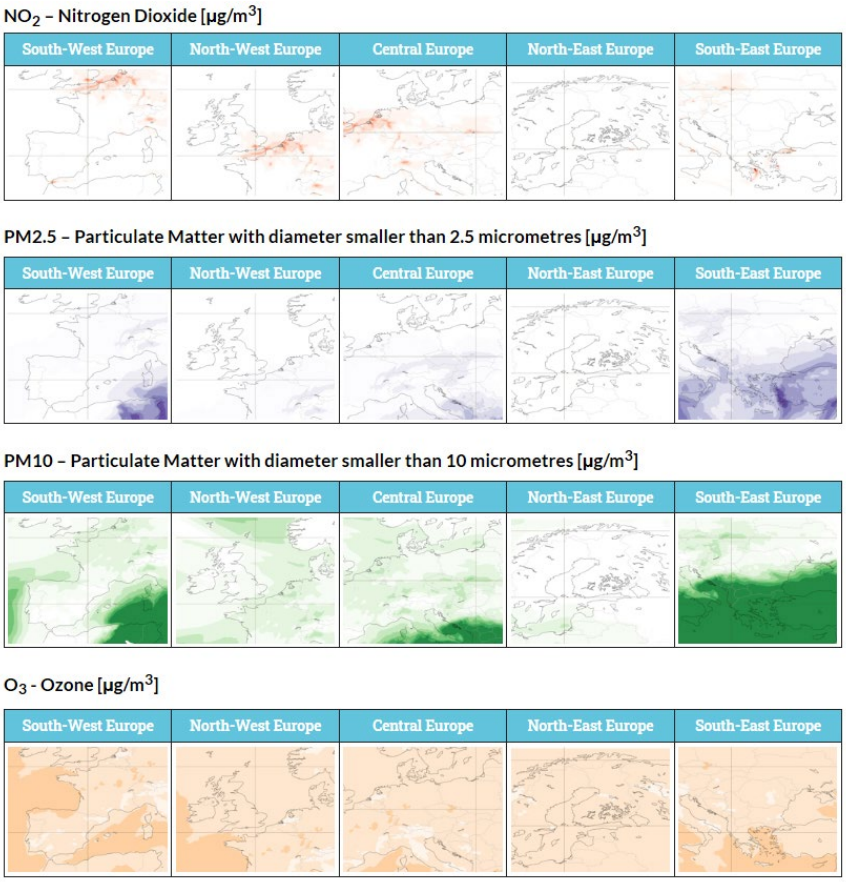

CAMS COVID resource maps. Maps available on the CAMS COVID resource showing air pollution across Europe. (Credit: Copernicus Atmosphere Monitoring Service / ECMWF)

January. In April and May, the data showed that most European countries had lower-than-usual levels of nitrogen dioxide and slightly lower fine particulate matter levels.

Since making the COVID resource public in March, CAMS has been looking more closely into possible links between air quality and COVID-19. The main questions that CAMS seeks to answer are whether short- and long-term exposure to air pollution are predictors for the outcome of the disease; to what extent particulate matter is involved in the spread of the disease; and what the effects of lockdown measures have been on air quality. CAMS is working with epidemiologists to investigate the first of these questions and in so doing is taking all necessary precautions around the use of personal medical data. CAMS hopes that the outcomes of these studies will help governments to implement strategies to manage possible future waves of COVID-19 in their countries, as well as to develop some longer-term strategies if the virus is here to stay.

C3S and COVID

Meanwhile, C3S has released an application that maps COVID-19 mortalities against temperature and humidity. It is known that other coronaviruses exhibit a strong seasonal cycle with outbreaks in winter and disappearance in the summer months. SARS-CoV-2 – which causes COVID-19 – is a new virus about which we know very little. That is why C3S is exploring how it could be affected by climate.

C3S developed the Monthly Climate Explorer for COVID-19 to make

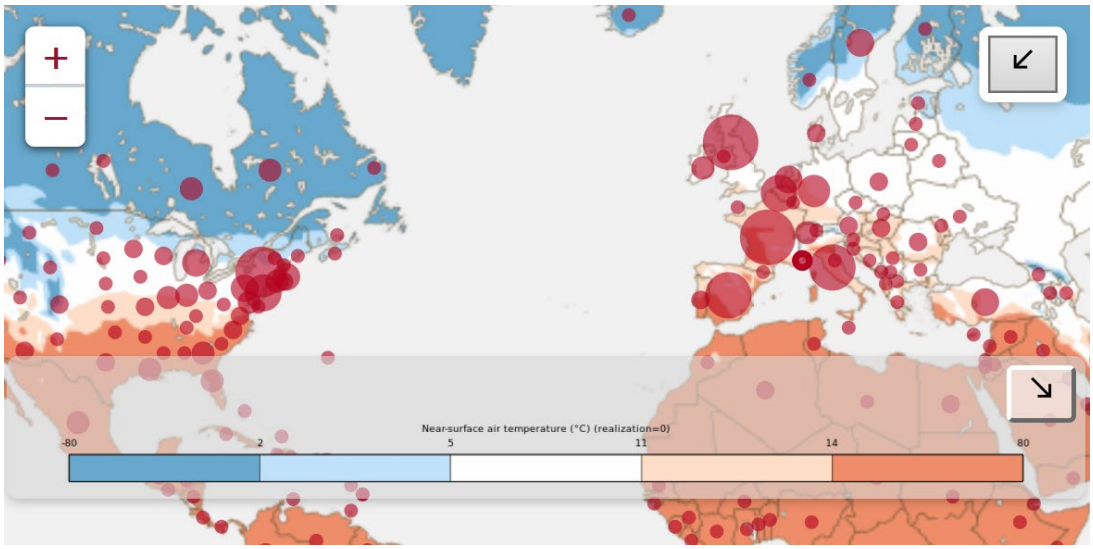

COVID-19 Climate Explorer: temperature and humidity. This screenshot from the C3S application shows COVID-19 mortalities and worldwide temperature for April 2020. White areas show regions where climate conditions are considered to be more conducive to the spread of coronavirus.

climate information more accessible to policymakers and health authorities. The questions that the app could help to answer include to what extent climate controls the intensity of the outbreak; how likely a second wave is to occur upon the arrival of the next winter season; and how current outbreaks may be correlated with air pollution. It is important to note that the significant COVID-19 outbreaks in warm Brazil and Mexico suggest that the impact of the climate on the spread of the virus is probably rather small, if it is present at all.

The first version of the app simply mapped the average temperature and humidity for each country or state against COVID-19 deaths for each month since January. It does seem to suggest that – at least in the initial phase of the pandemic – the largest outbreaks occurred in locations averaging around 10°C. Given the possible connections between air pollution and COVID-19 outbreaks, and taking advantage of the strong synergies that exist between C3S and CAMS, it was decided to add CAMS air quality information to the app. C3S also updated it to weight the average temperature, humidity and mortality data across each European country according to population density. This should give a better indication of the weather conditions most of the population have experienced during the outbreak. If a solid relationship between the spread of coronavirus infections and climate is confirmed, C3S forecasts of expected climate conditions for the coming months would help to provide guidance on the most suitable government interventions.

Copernicus COVID resources

CAMS COVID resource: *https://atmosphere.copernicus.eu/european-air-quality-information-support-covid-19-crisis*

C3S COVID Climate Explorer: *https://cds.climate.copernicus.eu/apps/c3s/app-c3s-monthly-climate-covid-19-explorer*

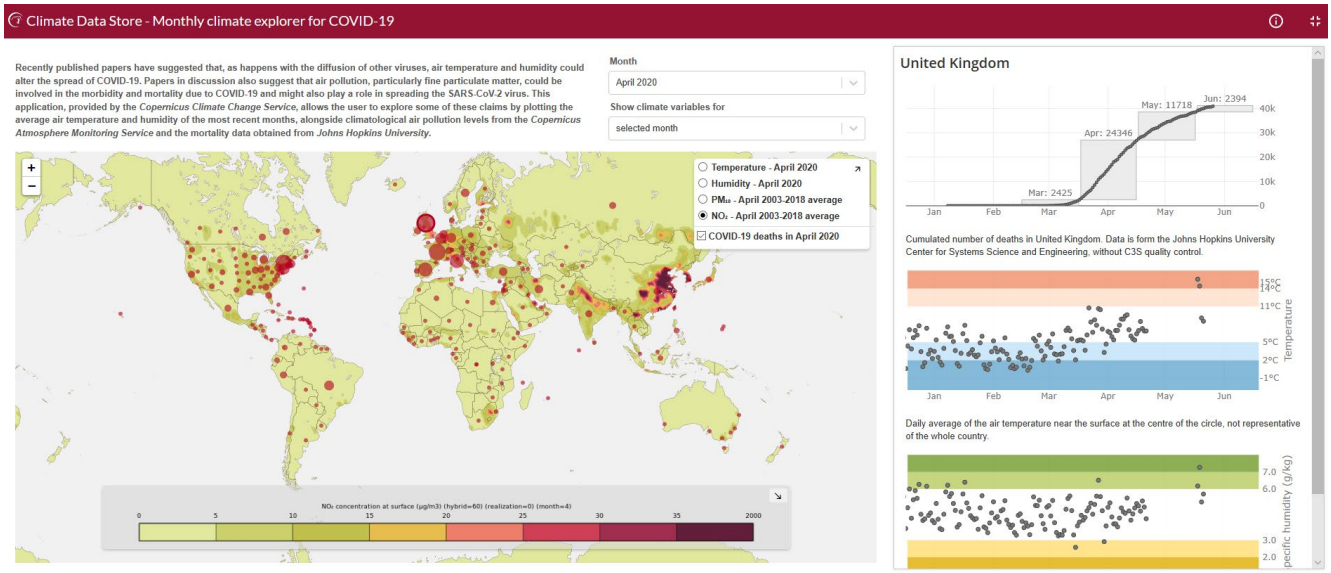

COVID-19 Climate Explorer: air quality. The Monthly Climate Explorer for COVID-19 application includes air quality information as well as temperature and humidity data. This screenshot shows mortality data mapped against nitrogen dioxide levels, and more specific data for the UK is shown on the right.

Coordinated response mitigates loss of aircraft-based weather data

Bruce Ingleby, Chris Burrows, Sean Healy

A coordinated response involving EUMETNET (a network of 31 European national meteorological services), national meteorological services and private companies has helped to mitigate any adverse effects of the COVID-19-related loss of aircraft-based observations on weather forecasts. In March and April, due to the COVID-19 pandemic, there was a sharp drop in flights and thus in the aircraft-based observations available to weather prediction centres. The continued availability of complete sets of satellite observations from EUMETSAT, ESA and other space agencies ensured that there was no severe impact from the loss of aircraft observations, as satellite data remain the most important observations. Aircraft reports include temperature and wind and in some cases humidity and turbulence. They are used together with many other observations to help estimate the state of the Earth system at the start of forecasts.

Responses to the drop in observations include the use of previously untapped aircraft-based observations; an increase in the number of radiosonde launches from some locations; and the assimilation of additional satellite data. In an example of successful collaboration with the private sector, the companies FLYHT and Spire stepped in to provide additional aircraft-based observations and radio occultation satellite data, respectively.

The impact

Between mid-March and mid-April, the number of aircraft reports received at ECMWF went down by about 75% before levelling out and then slowly picking up again. A data denial experiment run at ECMWF in 2019 suggested that removing all aircraft data has most impact at aircraft cruise levels (250–200 hPa or 10–12 km altitude). Here 12-hour wind and temperature forecasts became about 10% worse in the northern hemisphere extratropics. At the surface, 3- or 4-day forecasts of mean sea level pressure deteriorated by about 3% on average. There was, however, no clear signal in

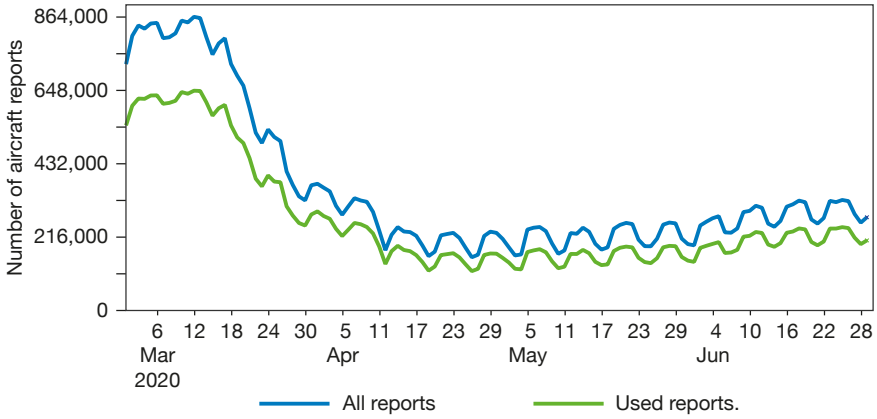

Numbers of global aircraft reports received at ECMWF per day. The regular dips reflect reductions in the numbers at weekends. There is some thinning and a small proportion of rejections so that the number assimilated (green) is less than the number received (blue). Most reports are received as part of the WMO's Aircraft Meteorological Data Relay (AMDAR) programme.

ECMWF forecast verification in April and May that could be linked to the decrease in aircraft numbers. Possible explanations are:

- Day-to-day and seasonal variability in forecast skill make it difficult to pin down the impact of reduced data availability
- The impact per observation increases somewhat with reduced data density, so one would expect to see less than 75% of the 'no aircraft' impact from the current configuration
- Additional data from a range of sources, partly made available in response to the drop in aircraft data, helped to mitigate any detrimental effects.

The response

EUMETNET has played a key role in coordinating the response to the loss of data among its members. It assessed the impact of the COVID-19 restrictions on the European Composite Observing System (EUCOS) and put in place a coordinated mitigation plan amongst EUMETNET members. Part of the response was to optimise and expand the use of aircraft observations that continued to be available:

- EUMETNET changed its configurations to make the most of any flights that E-AMDAR-equipped aircraft make. E-AMDAR is the EUMETNET AMDAR programme.
- In collaboration with EUMETNET and the UK Met Office, the company FLYHT made its aircraft observations available for free for a limited period of time. On 12 May, ECMWF started actively using some of these data.
- The European Meteorological Aircraft Derived Data Center (EMADDC) at the Royal Netherlands Meteorological Institute (KNMI) has been processing 'Mode-S' air traffic control signals to derive wind and temperature information. Following a recent meeting of experts, ECMWF has been working on processing the data and can now use them in a test version of the forecasting system (see separate article in this Newsletter).

In other developments regarding in-situ weather observations:

- Coordinated by EUMETNET, several of its members increased the frequency of radiosonde ascents from some of their stations. However, as the radiosonde figure shows, in

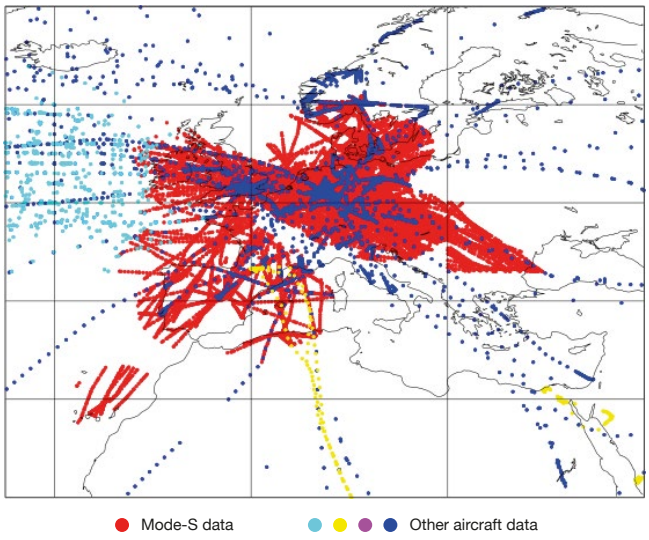

Twelve-hour Mode-S data coverage in a test system. Processing of 'Maastricht Area' Mode-S data covering the Netherlands and adjacent areas has been operational at KNMI for some time. The figure shows Mode-S aircraft-based 12-hour observation coverage from 21 UTC on 10 June 2020 over a much wider area in a test system. After ECMWF thinning, only about 5% of Mode-S reports are shown.

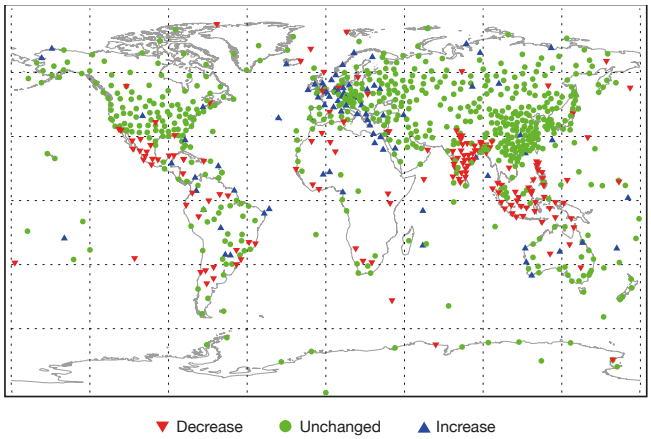

Radiosonde report availability. The chart compares the availability of radiosonde reports in May with that in March 2020.

some other places the numbers of radiosonde ascents dropped, perhaps due to supply difficulties.

- As part of a longer-term study, ECMWF is looking at the quality and possible assimilation of radiosonde descent data after balloon burst. In June 2020, ECMWF started the operational assimilation of most descent data from German radiosondes; the impact is currently modest as the numbers are relatively small, but it is expected to increase once descent data from other countries are assimilated too.
- In some areas, the number of surface reports from airfields (METARs) went down.
- In general, SYNOP weather station reports have stayed relatively constant.

At ECMWF, in normal times aircraft reports are second only to satellite data in their impact on forecasts. There are several recent additions to the satellite data assimilated at ECMWF which helped to make up for the loss of aircraft data:

- In 2019, ECMWF started assimilating data from several important instruments onboard EUMETSAT's Metop-C satellite.
- In January, ECMWF began to assimilate wind observations from ESA's ground-breaking Aeolus satellite.
- In March, the Centre started to use GNSS radio occultation (GNSS-RO) measurements from the FORMOSAT-7/COSMIC-2 mission, increasing the number of occultation profiles available for operational assimilation from around 3,000 a day to around 8,000.
- In mid-May, the number of occultations rose again by another 5,000 profiles a day when ECMWF began to assimilate RO data from the data and analytics company Spire.

Spire had offered to provide its RO observations free of charge for a limited period of time to help mitigate the loss of aircraft data. Building on previous work on the data by the European Space Agency (ESA), EUMETSAT and the UK Met Office, ECMWF was able to quickly move from quality assessment and passive monitoring to active assimilation. The additional RO data improved forecasts against a range of metrics. In terms of the relative impact of different types of observations on forecasts, between the end of March and the end of May aircraft-based observations went down substantially and RO data went up in broadly equal measure.

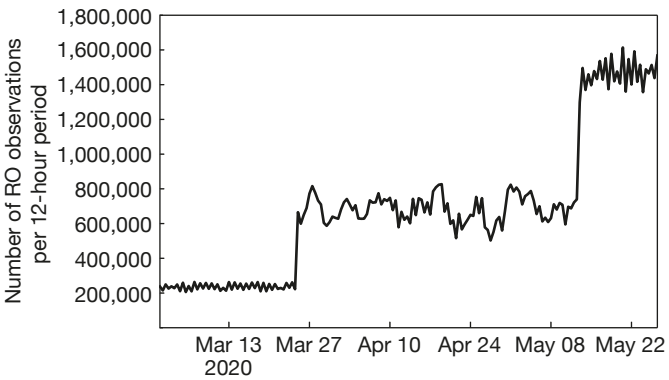

Number of radio occultation observations assimilated at ECMWF. The numbers shown in the chart are for individual observations. Each RO vertical profile contains between 250 and 300 such observations, which provide information on temperature and humidity. The step changes at the end of March and in mid-May mark the start of assimilating COSMIC-2 and Spire data, respectively.

EMADDC Mode-S: a new source of aircraft data over Europe

Bruce Ingleby (ECMWF), Jan Sondij, Siebren de Haan (both KNMI)

Mode-S aircraft data now provide high-density coverage of wind and temperature over large parts of Europe (see the figure in the preceding article). The Royal Netherlands Meteorological Institute (KNMI) has been working on Mode-S data for about ten years and the UK Met Office for almost as long. In recent years, a wider, more coordinated approach has been supported by EUMETNET and, partly funded by the EU, KNMI set up the European Meteorological Aircraft Derived Data Centre (EMADDC). EMADDC has an operational product centred on the Netherlands and a test product covering much of Europe. When the numbers of flights over Europe reduced dramatically in March and April, EMADDC consulted with its partners, suppliers and EUMETNET and decided to make the test product available to users for now. For the same reasons, ECMWF brought forward plans to process and assess the data.

What is Mode-S?

In some Air Traffic Control (ATC) regions, Mode-S Enhanced Surveillance (Mode-S EHS) reports are broadcast by aircraft in response to interrogation from ATC radar. These can be processed to derive wind and temperature. The quality of the wind data is similar to that of other aircraft reports, the temperature quality is somewhat worse because of the indirect reporting. The obvious feature of Mode-S data is the high data density: locally there can be about one hundred times more Mode-S than AMDAR reports. This is partly because of the high frequency of reports (up to every four seconds) and partly because almost all commercial aircraft have to respond, but only a subset provide AMDAR reports. Mode-S winds have been used in several limited-area forecasting systems.

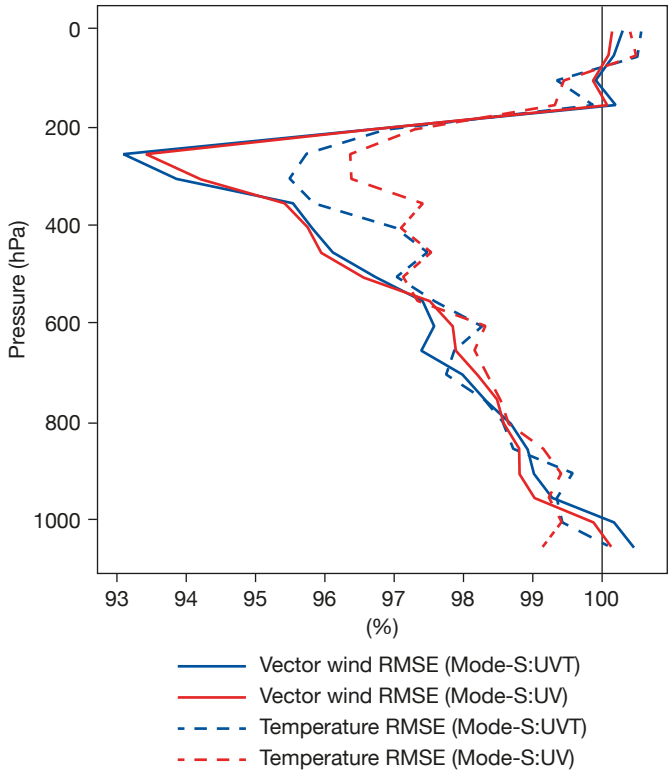

Fit of 12-hour forecasts to European radiosonde data. The chart shows the change in root-mean-square error (RMSE) of 12-hour forecasts of wind and temperature verified against radiosonde observations when Mode-S:UVT or Mode-S:UV data are assimilated, normalised by the control experiment without Mode-S data assimilation so that values less than 100 represent improvements. The data cover the period of 25 April to 26 June 2020.

Testing at ECMWF

ECMWF started to archive the data on 25 April and has since carried out testing and assimilation experiments after making various minor software changes. After using the standard thinning routine, about 4.5% of Mode-S reports were assimilated. One test assimilated the winds only (ModeS:UV), another assimilated the temperatures as well (ModeS:UVT). The largest impact is in the upper troposphere, as expected. Twelve-hour wind forecasts are improved by up to 6% compared to European radiosondes and up to 3 or 4% for temperatures. Most of the impact comes from Mode-S winds, while assimilation of Mode-S temperatures has very little effect on wind forecast scores but gives a slight improvement in upper tropospheric temperatures. We hope to start operational assimilation of Mode-S winds at ECMWF in July and to work on other aspects, such as the weighting and use of the temperatures, in the near future. As the number of aircraft flights recovers slowly, the numbers of both AMDAR and Mode-S reports over Europe will increase and the balance between them will be kept under review. There is also the prospect of acquiring Mode-S data from some other parts of the world, such as Australia.

Embracing the virtual challenge: UEF2020

Becky Hemingway, Anna Ghelli, Esperanza Cuartero

This year's Using ECMWF's Forecasts (UEF) meeting was held virtually from 1 to 4 June. The online meeting attracted 227 people from over 40 countries, many more than ECMWF has been able to accommodate at previous UEF events on its premises, increasing the reach of the event to the wide community of ECMWF users. This year's theme, 'Keeping users at the heart of operations', encouraged the exploration of end-user needs for users from all over the world. Participants discussed how weather and environmental information providers can meet those needs by delivering added-value outputs.

Users are key to everything that is done at ECMWF. Two-way communication between users and data providers and effective channels to collect feedback and advice are essential to ensure both parties can perform at their best. UEF2020 focused on four thematic areas: research to operations and operations to research; novel products and services; integrating new products in established processes; and user-focused planning.

In addition to plenary session talks, a variety of formats were used in the virtual environment: poster sessions, a User Voice Corner, Speakers' Corner talks, virtual breakout groups and interactive activities.

Meeting highlights

ECMWF Director of Forecasts Florian Pappenberger gave a presentation on current and future upgrades of the Centre's Integrated Forecasting System (IFS), improvements in forecast performance, Metview's new Python interface, and available learning and training resources. He also gave an update on the construction of ECMWF's new data centre in Bologna, Italy. Thomas Haiden (ECMWF) went into more detail on ECMWF's forecast performance, including substantial improvements due to IFS Cycle 46r1. He also talked about how COVID-19 has reduced the amount of aircraft data received, while pointing out that this has not had a major impact on performance scores.

Florian also highlighted that ECMWF is making a significant effort, through a number of initiatives, to support applications of artificial intelligence and machine learning and to identify how such applications may improve numerical weather prediction.

His remarks were complemented by David Hall's (Nvidia) presentation on 'Machine Learning for Weather', which clearly articulated the gains which can be made, by both data providers and users, by using machine learning in weather prediction.

Attendees were given an overview of the Research to Operations (R2O) process at ECMWF by Jenny Rourke and Michael Sleigh (ECMWF). They highlighted the many ways users can feed into the R2O process, including during UEF2020; provided examples of user feedback leading to improvements in operations; and asked participants for feedback using interactive polls.

A number of novel products, services and tools were presented throughout UEF2020, including using ECMWF ensemble products in tropical cyclone

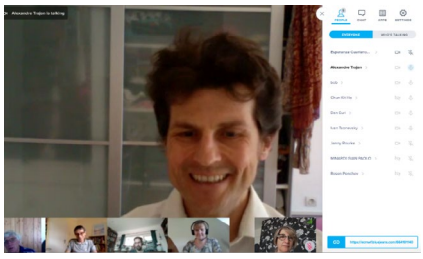

Informal meetings. Conversations over Coffee helped attendees to meet one another and provided a forum to discuss topics they were interested in.

The technology behind UEF2020

Running a fully online event poses challenges but also brings great opportunities and benefits, with technology helping to make it happen. Technology allowed ECMWF users from all over the world to attend the meeting; it allowed speakers to present their work without having to travel, thus reducing carbon footprints; and it enabled participants to play along with interactive sessions and provide feedback from their own homes.

ECMWF organisers created a website dedicated to the UEF which featured everything a participant needed to fully engage with the event. Plenary presentations were live-streamed with each presentation and poster having a dedicated page where comment boxes allowed conversations to continue throughout the event. Poster sessions were held using 'drop-in' virtual rooms where attendees could meet authors to discuss their work. The User Voice Corner used virtual breakout groups to have more focused discussions on specific topics. Conversations over Coffee meetings were held for participants to network during breaks, an important part of any event. Interactive sessions engaged the audience using walk-through demos that could be played with online and online apps which gathered valuable feedback.

field campaign planning and using seasonal data to optimise hydropower stations in South America. Thomas Leppelt (DWD) showcased his work using sub-seasonal data to forecast agricultural droughts with diagrams illustrating soil moisture forecasts and forecast skill in Germany. Richard Dixon (CatInsight, University of Reading) explored ECMWF's ERA5 reanalysis vs SEAS5 seasonal forecasts from an insurance loss forecast perspective, showing differences in loss model output when using windstorm data.

Poster presentation topics included Chun-Kit Ho's (Hong Kong Observatory) work on an informative global heatwave risk alert system; Roberta Amorati (ARPAE, Italy) showed how climate change affects air quality with a focus on particulate matter and ozone; and Biserka Frankovic (Croatia Control) presented a project providing graphical route forecasts of meteorological phenomena for aviation.

Popular UEF sessions such as User Voice Corner and Speaker's Corner still took place, albeit virtually. Tim Hewson (ECMWF) presented the outcomes of the User Voice Survey, which collected feedback on ECMWF products and services and asked users to suggest ideas for the future. Breakout groups then focused on specific topics, including extended-range (monthly) forecast products, precipitation forecast issues and ecCharts and meteograms. Speaker's Corner demonstrated new CAPE and CIN parameters, meteogram updates and tropical cyclone radius improvements.

The last morning of UEF2020 was dedicated to three EU-funded Copernicus Services in which ECMWF is involved, with talks on various

Positive feedback. Some of the feedback received from participants in UEF2020.

aspects of the Copernicus Climate Change Service (C3S) and the Copernicus Atmospheric Monitoring Service (CAMS), both implemented by ECMWF, and on the Copernicus Emergency Management Service (CEMS), to which the Centre contributes. Vincent-Henri Peuch (ECMWF) discussed changes in air quality across the globe due to COVID-19 using CAMS data, showing a decrease in nitrogen dioxide levels by over 50% in Madrid compared to forecasts without COVID-19. CAMS data is also used in Capgemini's AsSISt airline maintenance service, presented by Carine Saüt and Nicolas Estival, an innovative tool which provides indicators to airline companies and aircraft manufacturers of plane exposure to harmful, abrasive particles based on their flight path, allowing them to optimise maintenance and repair plans.

Attendees were pleased about the way in which UEF2020 had been organised online. Comments included: "Many thanks to all the organizers for making the UEF possible!", "Thanks a lot for this event, EC again proves it's a team of very innovative people!" and "This has set the standard for virtual conferences!". Positive feedback was received on the sessions and the opportunities to engage with ECMWF staff.

The most quoted word to describe UEF2020 was 'communication'. This is fitting as UEF's spirit has always been to facilitate two-way communication with users. All the presentations, posters and session recordings are available on the ECMWF website at: https://www.ecmwf.int/en/learning/workshops/using-ecmwfs-forecasts-uef2020

New Council President elected

Gen. Isp. G.A. Silvio Cau. ECMWF's Council elected Gen. Isp. G.A. Cau as its new President during its 96th session on 23 June 2020.

In June 2020, ECMWF's Council unanimously elected Gen.Isp. G.A. Silvio Cau of Italy as its President and Dr Daniel Gellens of Belgium as its Vice-President. Gen. Isp. G.A. Cau is the Head of the Italian National Meteorological Service and Dr Gellens is the Director-General a.i. of the Belgian Royal Meteorological Institute. Gen. Isp. G.A. Cau was previously the Council's Vice-President. He succeeds Juhani Damski, who was elected to the post of President in December 2019 but had to step down as he is leaving the Finnish Meteorological Institute. Council President and Vice-President appointments are for a one-year term of office with the possibility of re-election no more than twice in succession.

ECMWF training – responding to new challenges

Sarah Keeley, Anna Ghelli, Iain Russell

ECMWF's training courses in 2020 have been and will continue to be very different from previous years, mainly because of the need to run them virtually. Despite this, ECMWF has continued to deliver its training programme. Learning activities in the first half of 2020 took place either as blended courses or completely online, providing training to 270 people. Two thirds of the participants came from Member and Co-operating States.

NWP courses

At relatively short notice this year, we took the decision to run the numerical weather prediction (NWP) courses virtually due to the COVID-19 pandemic. The situation changed dramatically within the six-week window in which the NWP courses were run. The data assimilation course was run virtually and face to face to allow those who did not wish to travel to stay at home; the subsequent satellite data assimilation and numerical methods courses were given virtually from the classroom at Shinfield Park, so the lecturers were in familiar surroundings; and finally, the predictability and parametrization courses were run from everyone's homes, with some lecturers having to give lectures in cramped conditions to avoid interruptions from the smallest members of their family! We made the difficult decision to postpone the newly created course 'A hands-on introduction to NWP models: understanding and experimenting' until we can run this course face to face. There is such a large amount of practical work, including getting into the details of running code, that we felt the online experience would not allow participants to meet their learning objectives. Face-to-face discussion with experts and practical work seemed essential to this task.

Online training. In 2020, many courses have been delivered virtually for the first time.

For the virtual NWP courses, this meant a big component of the learning and networking in the course was lost; often the practical sessions are where participants consolidate their learning and have an opportunity to query things one on one with the lecturers. The lecturers tried to recreate this as best as possible and took time to answer individuals' questions after lectures. The question sessions often ran into the coffee breaks as people had so much to ask. The online experience has highlighted the value face-to-face training provides in terms of opportunities for early-career scientists, or those new to the field, to build their own network and gain a deep understanding of the training material. The informal conversations where random connections are made, or a new idea is sparked, over lunch or a drink at the end of a long day, were sorely missed by lecturers and participants alike. This is very hard to recreate online. However, this year the Using ECMWF's Forecasts meeting (UEF) has explored new innovative ways to host a networking event online, and the article by Becky Hemingway, Anna Ghelli and Esperanza Cuartero in this Newsletter showcases what is possible.

Feedback from participants

Despite the many changes at short notice the feedback from the participants in NWP courses has been great: they have really appreciated having something else to focus on than the lockdown and the pandemic. It was clear from the comments that the lectures were still well received. Here is a selection:

"I don't remember having ever visited a course with so many outstanding lectures. Thank you so much!"

"I was impressed with how well the virtual course was put together. It's a shame we weren't able to take part in the practical aspects of the course but given the circumstances I think it was very well done."

"Under the circumstances, I was extremely impressed with the quality of online lectures. I did encounter some technical issues, but the overall quality was well above any video conferencing/large groups I have previously taken part in. The lecturers were all brilliant and coped very well with lecturing online."

Learning management platform

Participants can now log their learning through our new learning management platform. This allows us to track pre-course learning to make sure everyone has a similar level of background knowledge before attending a training event, and it enables learners to study at their own pace. It is a great central hub for all our learning resources. Registered users can access the learning management platform here: *http://learning.ecmwf.int/*.

For details on all training courses, visit: *https://www.ecmwf.int/en/learning/training*.

Other courses

ECMWF has a tradition of offering virtual learning events. These happen throughout the year, with a recurrent appointment for a computing and software online training week in the spring. The current pandemic did not significantly disrupt the Metview training plans as for the second year running two webinars were given. This year, the topics were the interactive analysis of data and the processing of

ensemble data. The sessions were recorded and Jupyter notebooks with Python source code made available.

In the second half of 2020, the traditional Use and Interpretation of ECMWF products course will take place. This is a blended course, but this year it will need to run completely online. The practical activities will be run using virtual classrooms where participants, in groups of five or six, will explore the use of ECMWF products in real-life case studies supported by a trainer. We are looking forward to this course and the opportunities it offers. We will be able to provide training to a wider audience than before as in the blended version we have an upper limit of 25 participants.

User workshop aids European Weather Cloud development

Stephan Siemen, Xavier Abellan, Cristian Simarro (all ECMWF), Joachim Saalmüller, Mike Grant, Jörg Schulz (all EUMETSAT)

A joint EUMETSAT-ECMWF workshop on use cases for the European Weather Cloud was held on 27 May 2020. During the pilot phase of the European Weather Cloud, use cases are an important way for us to work with Member States to develop the future cloud service. The workshop attracted much interest in our Member States with over 200 registrations and over 185 participants online at peak times.

The workshop was split in three sessions:

- In the first session, the two user support teams involved at EUMETSAT and ECMWF gave an overview of the capabilities of the current system. They also showed how users can access the system.
- The second session presented five use cases on the cloud. They included the support given to Croatia after the recent earthquake both on the EUMETSAT and ECMWF side, the hosting of the Dutch national meteorological service's Climate Explorer and the development of a Jupyter-based platform to enable machine learning research in cooperation with the University of Oxford.
- The third session allowed participants to ask questions and to discuss feedback from the use cases. The feedback from the audience was very positive and gave very valuable input for upcoming developments on the cloud. Thanks also to the sli.do Q&A system used in parallel, over 46 user questions on usage of the cloud could be collected and answered.

Workshop participants. The European Weather Cloud workshop took place online due to COVID-19 restrictions.

Outcome of the Q&A discussion

Most of the 46 questions and comments received in the Q&A session were related to technical aspects. These questions covered areas from the basic setup to more advanced topics, e.g. on technical solutions for container orchestrations. These questions were addressed by technical staff attending the session at the time. A group of questions concerned data access. This is unsurprising since fast and localised access to large datasets is the main advantage of the European Weather Cloud. Comments from participants showed that there is interest in harmonising access between EUMETSAT and ECMWF. Some questions enquired about how to get access to and host services on the system. These, and some more direct questions on documentation, showed that the joint Service Desk space and documentation for the European Weather Cloud needs to be advertised more widely.

More information about the meeting, including presentations and records of the Q&A session, can be found on the meeting web page: https://bit.ly/2BpWbRm. The plan is to repeat such workshops every six months, and the next one is scheduled for November 2020.

Introducing Sites: static websites as a service

Manuel Martins

'Sites' is a new service that allows ECMWF staff to create and expose static content, internally or externally, in a secure, uniform and reliable way without any technical support. A static website does not use any external database and is fully coded in Hypertext Markup Language (HTML) and Cascading Style Sheets (CSS), using JavaScript and images, where changes are rare, making it easy to cache.

Motivation

ECMWF provides a vast range of web services for multi-purpose use. These include tools such as Drupal, Confluence, FTP, Microsoft Teams, etc. But there are occasions when people need to host HTML or large files on a web server and expose these both internally and externally. Such content is not necessarily suitable for the existing services. As a result, over the years it has often been disseminated through unsuitable channels or has been misplaced, making it difficult to identify, access and manage.

Many ECMWF staff currently host, in one form or another, a website for their own convenience. This enables them to share, within a team or department, charts, experimental results, benchmarking etc. However, many of these websites are run on desktops, which results in a lack of internal and external exposure, conventional subdomains, security, proper storage, monitoring, etc. Use cases identified over the years include:

- Sharing static charts, results or reports with internal and external users
- Storing or providing eLearning content
- Storing or sharing documentation such as reference manuals
- Storing content from legacy services
- Sharing large files accessed over HTTPS from a web interface.

These use cases were consolidated while gathering requirements for the migration of computing services and facilities to ECMWF's new data centre under construction in Bologna, Italy.

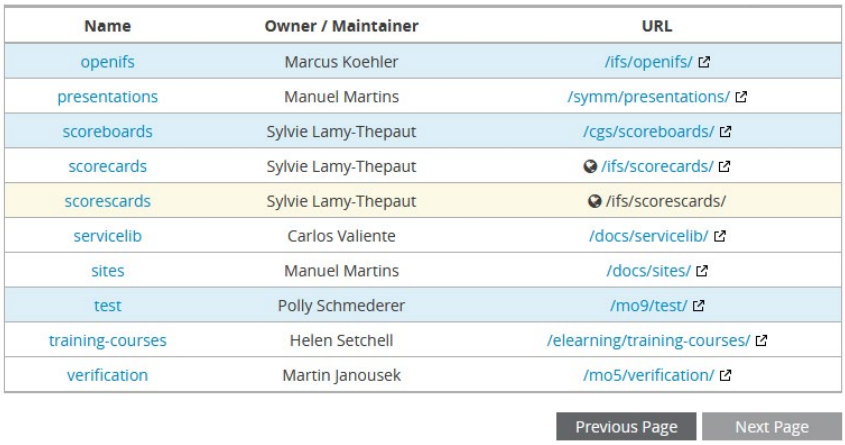

Name	Owner / Maintainer	URL
openifs	Marcus Koehler	/ifs/openifs/
presentations	Manuel Martins	/symm/presentations/
scoreboards	Sylvie Lamy-Thepaut	/cgs/scoreboards/
scorecards	Sylvie Lamy-Thepaut	/ifs/scorecards/
scorescards	Sylvie Lamy-Thepaut	/ifs/scorescards/
servicelib	Carlos Valiente	/docs/servicelib/
sites	Manuel Martins	/docs/sites/
test	Polly Schmederer	/mo9/test/
training-courses	Helen Setchell	/elearning/training-courses/
verification	Martin Janousek	/mo5/verification/

Previous Page Next Page

Sites Hub screenshot. The Sites Hub helps users to find sites of interest through a free text search facility.

How it works

Over the last few months, a platform to support these requirements has been developed on top of the application deployment and management platform Kubernetes, following a cloud native approach. The main portal, the Hub, is a centralized application which aggregates and manages all websites. Here, it is possible to navigate through the list of all available websites. Each website is independent and has its own web server, web application programming interface (API), web administration interface and storage. The web API and web administration interface are the content management tools and allow users to update the website whether they are running automated tasks (using the web API) or simply dragging and dropping files (using the web administration interface).

A website can be either private or public. If a website is private, proper authorisation will be needed to access its contents. Each website can be configured with a list of users or policies/groups that can manage and/or view the content of that website. Users log in using their ECMWF credentials. Creating new websites is quick and easy. All requests for new websites are validated by ECMWF's web management team and in some cases users might be redirected to a more appropriate service. A retention date is specified as part of the website creation process and is reviewed once it has expired. This is important in cases where the website has a pre-defined lifetime, e.g. because it is linked to a project. The site can then be decommissioned soon after.

Current status

Sites has been in production since April 2020 and currently hosts more than 20 websites, some of which are operational while others are just proofs of concept.

Some of the public websites that have already been migrated to Sites are:

- IFS Scorecards - https://sites.ecmwf.int/ifs/scorecards/
- Atlas Documentation - https://sites.ecmwf.int/docs/atlas/
- ecCodes Documentation - https://sites.ecmwf.int/docs/eccodes/

Useful links

List of Sites:
https://sites.ecmwf.int/list/

About Sites:
https://sites.ecmwf.int/about/

Sites documentation:
https://confluence.ecmwf.int/display/UDOC/Sites

IFS upgrade greatly improves forecasts in the stratosphere

Michael Sleigh, Philip Browne, Chris Burrows, Martin Leutbecher, Thomas Haiden, David Richardson

On 30 June 2020, ECMWF implemented a substantial upgrade of its Integrated Forecasting System (IFS). IFS Cycle 47r1 includes changes in the forecast model and in the data assimilation system. The upgrade has had a small positive impact on forecast skill in medium-range and extended-range forecasts in the troposphere and a large positive impact on analyses and forecasts in the stratosphere. The latter is mainly due to reduced large-scale biases.

Cycle 47r1 is the culmination of work from many ECMWF staff and it brings several changes. The main ones are:

- **in data assimilation:** revised model error in weak-constraint 4D-Var data assimilation; situation-dependent skin temperature background error variances from the Ensemble of Data Assimilations (EDA); shorter time step in the last 4D-Var minimisation; first guess in delayed cut-off 12-hour 4D-Var obtained from 8-hour Early Delivery Data Assimilation
- **in the use of observations:** revised ATMS (Advanced Technology Microwave Sounder) observation errors; spline interpolation introduced in the 2D GPS-RO (radio occultation) bending angle operator
- **in the forecast model:** quintic vertical interpolation in semi-Lagrangian advection; modified Charnock parameter for high wind speeds in tropical cyclones; 6-component MODIS (Moderate Resolution Imaging Spectroradiometer) albedo over land.

Data assimilation

In Cycle 47r1, the covariances controlling the model bias estimate in weak-constraint 4D-Var have been revised. The previous weak-constraint 4D-Var corrected only a small fraction of the model bias above 40 hPa, while the revised weak-constraint implementation better corrects the diagnosed cold and warm biases of the model above 100 hPa, reducing the mean error by up to 50%. Results show that biases in the upper stratosphere between 11 hPa and 1.5 hPa are also significantly reduced in the new system. For more details, see Laloyaux & Bonavita (2020).

Another important contribution to Cycle 47r1 is a change in the estimate of the background error variance for skin temperature over land, from constant values to spatially varying, situation-dependent variances derived from the EDA. This affects the assimilation of microwave and infrared (IR) radiance observations of the mid- and lower troposphere, which typically contain a contribution of radiation emitted from the surface. The EDA estimate was activated over land surfaces initially, where the magnitude of skin temperature errors can be very heterogeneous in space and time.

The time step in the last 4D-Var minimisation has been reduced in this new cycle from 900 seconds to 450 seconds. With this change, the inner loop and outer loop time steps match. This avoids different gravity wave speeds between the tangent-linear model (used in the computation of the final increment as part of the last inner loop) and the nonlinear model (outer loop). In the semi-implicit advection scheme of the IFS, the gravity wave speed depends on the time step. The change brings multiple benefits: clear improvements to stratospheric analyses and forecasts, and a smaller but statistically significant impact on tropospheric skill; monotonic convergence of incremental 4D-Var in some atmospheric situations, such as sudden stratospheric warming events; and an improved initial balance of the 4D-Var analysis.

The concept of continuous data assimilation introduced in Cycle 46r1 has been extended by using the analyses from each 8-hour Early Delivery Data Assimilation (DA) window as first guesses for the 12-hour Long-Window Data Assimilation (LWDA). From Cycle 47r1, the LWDA analysis can be viewed as a time extension of the DA analysis. There is no change in the background state for the LWDA, but the first minimisation is provided with a more accurate starting point. For more details, see Hólm et al. (2020).

As a result of this change, the analysis increments in LWDA increase, mainly due to the fact that more information is extracted from observations. This leads to an apparent degradation of forecasts when they are verified against own analyses. In reality, forecasts have not deteriorated but the analysis against which they are assessed has changed. When verified against an independent analysis, like reanalysis, the impact on

doi: 10.21957/b72xo6ms93

forecast skill from this change is neutral overall. An important benefit of this change is that it allows 4D-Var to more effectively initialise non-linear processes. Short-range forecasts are closer to observations in particular for observations which are more non-linearly related to the model state, such as radiances sensitive to water vapour, cloud and precipitation.

Use of observations

The use of hyperspectral IR data (AIRS, IASI, CrIS instruments) has been enhanced in Cycle 47r1 by allowing high-peaking channel radiances to be assimilated in locations where lower-peaking channels are rejected due to aerosol contamination. Up to Cycle 46r1, the aerosol detection scheme rejected entire IR spectra if aerosol was detected in any channel. The number of assimilated IR observations has increased by up to 5% for stratospheric channels due to this enhancement. The change is most effective in regions where aerosol (particularly Saharan dust) occurs most frequently.

In Cycle 47r1, a consistent formulation of the inter-channel error correlations was introduced for ATMS from the Suomi-NPP and NOAA-20 satellites. This change results in small but consistent improvements to first-guess fits to independent observations such as AMSU-A and the IR humidity sounding channels, indicating improved short-range forecasts of tropospheric temperature and humidity.

From Cycle 47r1, a bilinear interpolation replaces the nearest-neighbour interpolation in the computation of forecast departures for all-sky microwave radiance observations for most variables. These include temperature and humidity but not cloud hydrometeors and not the land–sea mask, for which nearest-neighbour interpolation is preferable. This change results in significantly improved first-guess fits to all-sky microwave imager and sounder radiances.

In Cycle 47r1, an improved interpolation approach has been introduced in the GPS-RO observation operator for bending angles. This revision of the interpolation ensures that refractivity gradients are continuous in the vertical and produce more realistic profiles of bending angle variability. The change leads to a small increase in the standard deviation of GPS-RO first guess departures due to the intended increase in variability, but the analysis departures are slightly improved.

Forecast model

In Cycle 47r1, the advection of temperature and humidity has been changed by increasing the order of the vertical interpolation in the semi-Lagrangian scheme from three to five. This quintic interpolation in the semi-Lagrangian advection alleviates an unphysical cooling of the IFS model in the stratosphere at high horizontal resolution. The change and its impact are described in detail in Polichtchouk et al. (2020).

A number of improvements have been made to the specification of the shortwave albedo of the land surface, snow and sea ice. The land-surface albedo is based on a monthly climatology derived from the MODIS instrument. Until Cycle 46r1, it consisted of separate albedos for direct and diffuse solar radiation in two spectral regions: ultraviolet/visible, and near-IR. Albedo for direct solar radiation was computed assuming an overhead sun, for which albedo is systematically lower than for other sun angles. In Cycle 47r1, the dependence of the direct albedo on solar zenith angle is represented following Schaaf et al. (2002). This requires six climatological fields, three in each of the two spectral regions. This tends to increase the albedo of snow-free land surfaces, on average. In addition, the albedo for the 0.625–0.778 μm band of the shortwave radiation scheme has been determined by a weighted average of the MODIS albedos for the ultraviolet/visible and the near-IR, instead of using the latter only. The improved albedo for this spectral band justified the removal of an artificial adjustment of the limits of the prognostic snow albedo, and the introduction of spectrally varying snow albedos consistent with MODIS observations as reported by Moody et al. (2007). These changes warm summer land areas in the model by around 0.1°C and by up to 0.3°C over North Africa, primarily due to the darkening of the land surface from the recomputed albedo in the 0.625–0.778 μm band. There is a small reduction in the root-mean-square error of temperature forecasts, which stems from a reduction in the model's cold bias in 2-metre temperature in many regions. A clear improvement in daytime temperature forecasts over the Sahara has been observed.

Two additional changes were made in the treatment of radiation: (i) the time series of total solar irradiance has been updated using data from Matthes et al. (2017), which include the 11-year solar cycle and are consistent with the latest solar measurements; (ii) the time series of concentrations of greenhouse gases have been updated (CMIP6's SSP3-7.0 / option 2). There is no detectable impact of (i) on forecasts, while (ii) slightly warms the upper stratosphere in analyses and forecasts in present-day simulations because in Cycle 47r1 CO_2 concentrations are consistent with recent measurements and slightly lower than previously used estimates of CO_2 concentrations.

The parametrization of momentum exchange with the ocean surface has been changed in Cycle 47r1. The relationship is expressed in a wind-speed-dependent drag coefficient. A considerable reduction of the drag under very strong winds (above 33 m/s) has

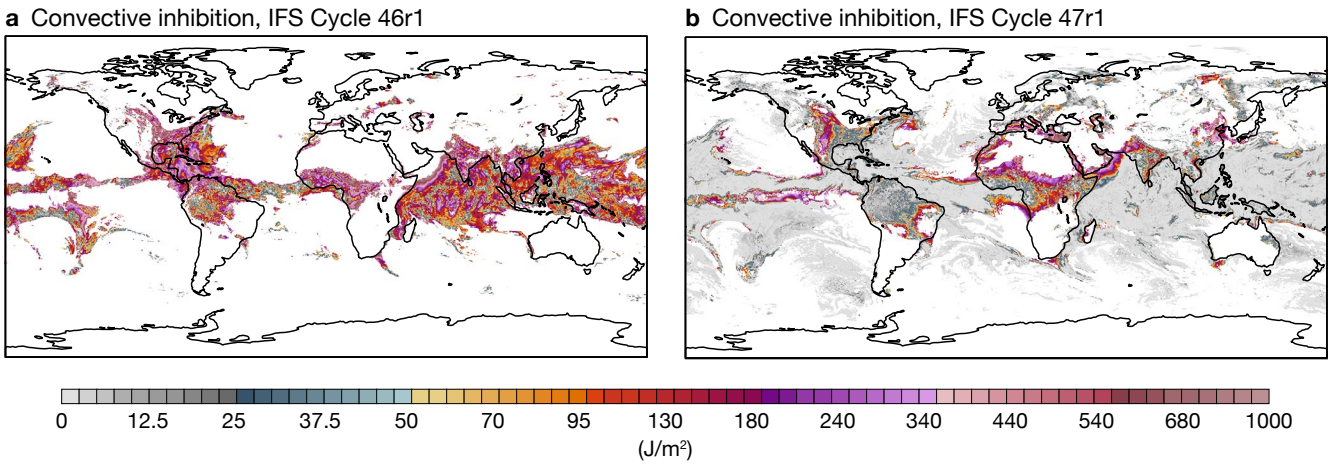

FIGURE 1 Three-day forecast of convective inhibition (CIN) valid at 00 UTC on 7 June 2020 for (a) IFS Cycle 46r1 and (b) IFS Cycle 47r1.

been introduced. This change of drag over the ocean at high wind speeds yields a substantial improvement in maximum 10-metre wind speeds in intense tropical cyclones. For more details, see the article 'Enhancing tropical cyclone wind forecasts' in this Newsletter.

Minor changes have been made in the convection scheme in Cycle 47r1. They involve stability corrections to the mid-level and deep convective closures and reduced bounds for parcel perturbations. Furthermore, the convective inhibition diagnostic (CIN) has been revised to use virtual potential temperature instead of equivalent potential temperature. The revised CIN is now much reduced and is closer to values expected by forecasters (Figure 1).

Impact on medium-range forecasts

Figures 2 and 3 show score changes and their statistical significance for the ensemble forecast (ENS) and the high-resolution forecast (HRES), respectively. HRES is run at TCo1279 resolution (corresponding to a horizontal grid spacing of about 9 km) and ENS at TCo639 (corresponding to a horizontal grid spacing of about 18 km).

The new cycle brings improvements throughout the troposphere in the order of 0.5% in extratropical forecasts. The improvements are most apparent in ENS scores, both against own analysis and against observations. In the extratropical stratosphere, the new cycle brings large improvements, such as 2–5% error reductions for temperature and geopotential at 100 hPa, and 5–15% at 50 hPa. In the tropics, there is an apparent degradation of 1–3% in upper-air scores when forecasts are verified against the new cycle's own analyses. This does not reflect any change for the worse in the forecasts but is the result of changes to the analysis, as described above. Verification against observations shows that upper-air changes in the tropics are neutral overall, with small improvements and deteriorations balancing each other out. One exception is 250 hPa temperature in the tropics, where a deterioration of 1–3% is seen against observations. This is mainly due to a small (about +0.1 K) shift in the mean, resulting from the model changes.

The new cycle improves forecasts of several near-surface parameters, most notably 2-metre temperature and humidity (by about 0.5–1%) both in the extratropics and, when verified against observations, also in the tropics. Extratropical 10-metre wind in HRES is slightly improved, as well as total cloud cover in ENS and HRES. Tropical 10-metre wind and precipitation are slightly deteriorated. Significant wave height is mostly neutral against observations and improved against own analysis.

Impact on extended-range forecasts and model climate

The impact of Cycle 46r1 on the model climate in the extended range (up to 46 days ahead) was generally neutral. By contrast, Cycle 47r1 has a significant positive impact in the lower stratosphere, with a decrease of the cold bias in the tropics at around 50 hPa. The impact of Cycle 47r1 on weekly mean anomalies is neutral, except for some improvement in 50 hPa meridional wind, and a slight, but statistically significant, degradation in week 1 in the tropics for upper-level fields. The degradation in the fair CRPSS is consistent with a slight reduction of ensemble spread in week 1 over the tropics.

In addition to monitoring the evolution of probabilistic forecast skill scores in the scorecards, it is important to monitor the predictive skill of sources of sub-seasonal predictability, such as the Madden–Julian Oscillation (MJO). The difference in MJO bivariate correlation between Cycle 47r1 and Cycle 46r1 is not statistically significant. However, in Cycle 46r1, the MJO was too weak compared with the ERA5 reanalysis (by about

47r1 ENS Scorecard

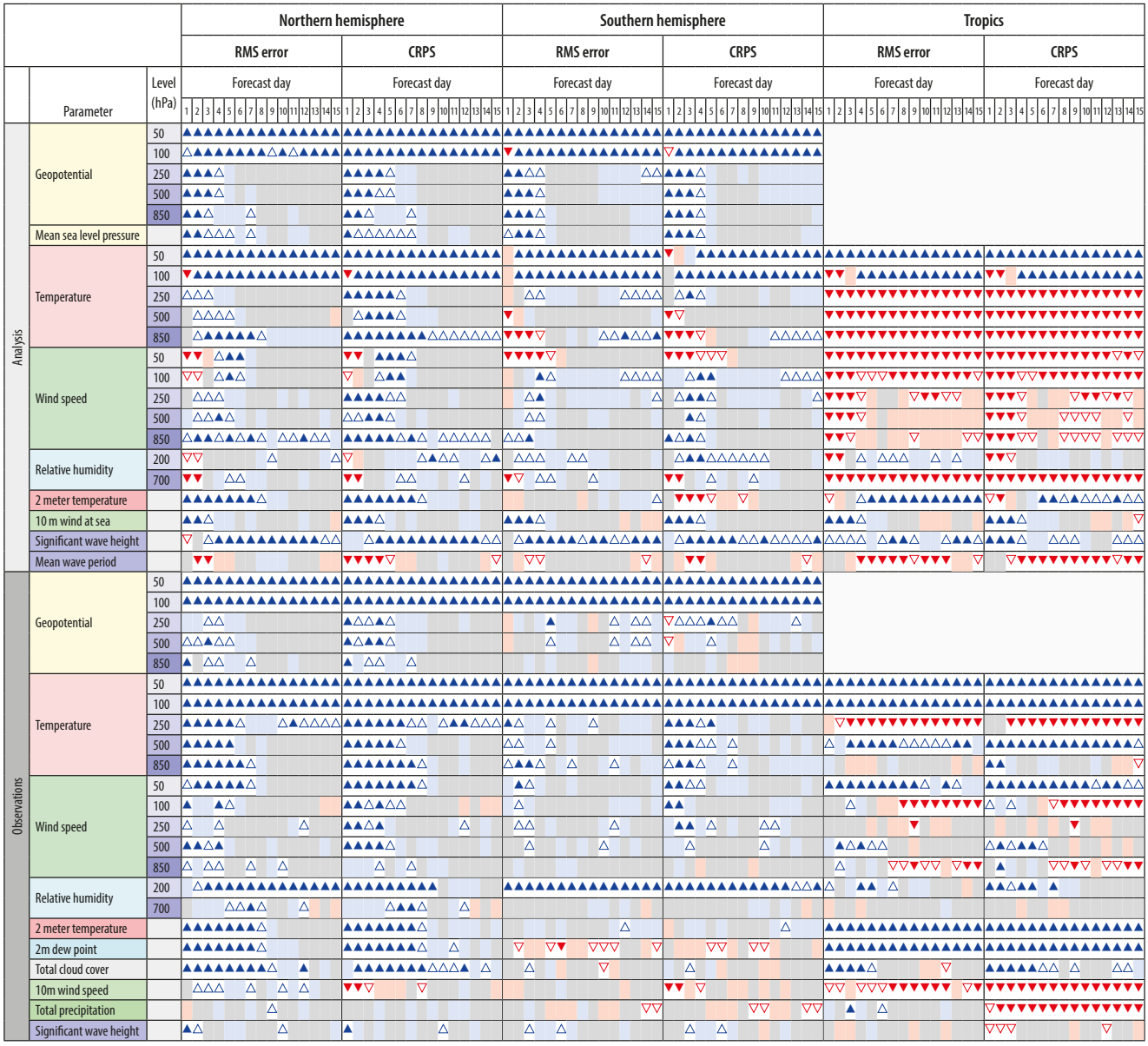

Symbol legend: for a given forecast step...

- ▲ 47r1 better than 46r1 statistically significant with 99.7% confidence
- △ 47r1 better than 46r1 statistically significant with 95% confidence
- 47r1 better than 46r1 statistically significant with 68% confidence
- no significant difference between 46r1 and 47r1
- 47r1 worse than 46r1 statistically significant with 68% confidence
- ▽ 47r1 worse than 46r1 statistically significant with 95% confidence
- ▼ 47r1 worse than 46r1 statistically significant with 99.7% confidence

FIGURE 2 ENS scorecard of IFS Cycle 47r1 versus IFS Cycle 46r1 for medium-range forecasts up to forecast day 15, verified by the respective analyses and observations at 00 UTC based on 350 ENS forecast runs in the period December 2018 to April 2020.

20% after day 15), and Cycle 47r1 weakens the MJO further by 3–4% in the extended range.

The seasonal forecast is not changed with Cycle 47r1. Nevertheless, the impact of the model upgrade on the model climate has been evaluated in lower-resolution seasonal forecasts. The most marked impact on the model climate in the seasonal range comes from introducing quintic vertical interpolation. This warms the equatorial and winter-hemisphere model climate stratosphere by about 0.5 K from the tropopause

47r1 HRES scorecard

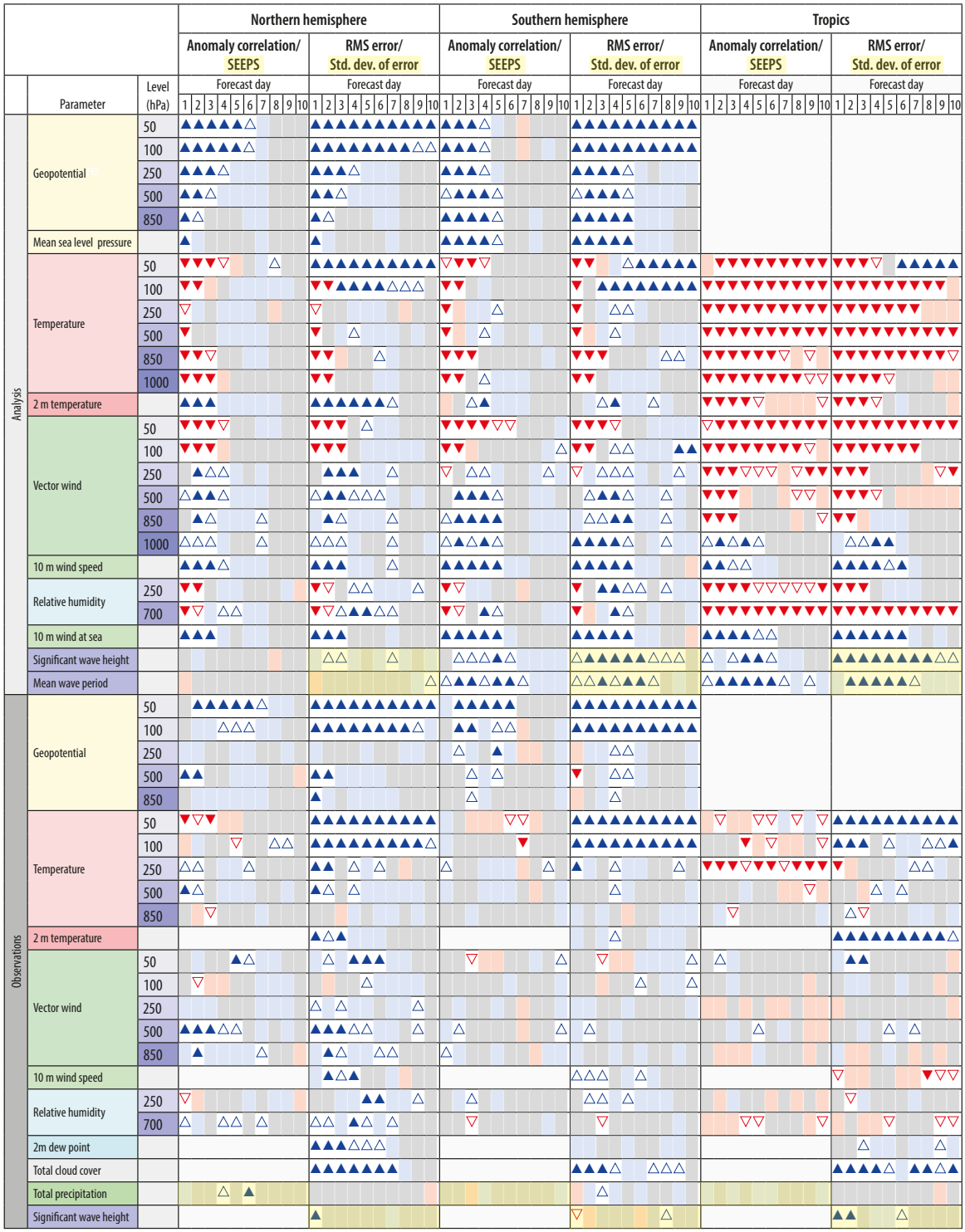

Symbol legend: for a given forecast step...

- ▲ 47r1 better than 46r1 statistically significant with 99.7% confidence
- △ 47r1 better than 46r1 statistically significant with 95% confidence
- 47r1 better than 46r1 statistically significant with 68% confidence
- no significant difference between 46r1 and 47r1
- 47r1 worse than 46r1 statistically significant with 68% confidence
- ▽ 47r1 worse than 46r1 statistically significant with 95% confidence
- ▼ 47r1 worse than 46r1 statistically significant with 99.7% confidence

FIGURE 3 HRES scorecard of IFS Cycle 47r1 versus IFS Cycle 46r1, verified by the respective analyses and observations at 00 and 12 UTC, based on 630 forecast runs in the period December 2018 to April 2020.

throughout the lower stratosphere, reducing the cold bias. Changes to the model physics have resulted in a small increase in precipitation in the Intertropical Convergence Zone (ITCZ) year-round. Longstanding biases in boreal summer zonal 10 m wind in the Indian Ocean increase slightly, worsening eastern equatorial Indian Ocean sea-surface temperature biases.

Forecast outputs

In addition to the change to convective inhibition diagnostic (CIN) described above, some other changes to the forecast outputs have been introduced with the implementation of Cycle 47r1.

The Extreme Forecast Index (EFI) for CAPE and CAPE-SHEAR now better represents 24-hour maximum values by sampling hourly values throughout the period (instead of the previous 6-hourly values).

New diagnostics of tropical cyclone (TC) size are introduced to supplement the existing forecasts of TC track and intensity (minimum central mean sea level pressure and maximum wind around a TC). TC size is represented by 'wind radii', which denote the furthest distance (in metres) away from the centre of the TC at which mean 10 m wind speed thresholds (34, 50 and 64 knots) are exceeded. Each of these are computed for each of four Earth-relative quadrants, i.e. NE, SE, SW and NW, delivering a total of 12 'size metrics' for each TC at each time step. More details are provided by Bidlot et al. (2020) in this Newsletter.

Summary

ECMWF's ten-year Strategy 2016–2025 describes two major avenues for further improvements in medium-range forecast skill. One is a more accurate estimation of the initial state and the consistent representation of uncertainty associated with observations and the model. The second is a better representation of model dynamics and physical processes, including interactions between different Earth system components. Cycle 47r1 includes developments in both areas. On the initial state side, it includes the revised weak-constraint 4D-Var scheme and matching time steps in the final 4D-Var outer loop, among other changes. On the modelling side, the new cycle includes quintic vertical interpolation in semi-Lagrangian advection, a modified Charnock parameter for high wind speeds occurring in tropical cyclones, and six-component MODIS albedo over land, among other changes.

The new cycle increases the forecast skill in the order of 0.5–1% in the troposphere and for some near-surface parameters, such as temperature and humidity, in the extratropics. The largest and most significant improvements from the new cycle are seen in the stratosphere, where a number of contributions have combined to address known model biases.

Further reading

Bidlot, **J.-R.**, **F. Prates**, **R. Ribas**, **A. Mueller-Quintino**, **M. Crepulja** & **Frédéric Vitart**, 2020: Enhancing tropical cyclone wind forecasts, *ECMWF Newsletter* **No. 164**.

Hólm, **E.**, **S. Lang**, **P. Lean** & **M. Bonavita**, 2020: Continuous long-window data assimilation, *ECMWF Newsletter* **No. 163**, 12.

Laloyaux, **P.** & **M. Bonavita**, 2020: Improving the handling of model bias in data assimilation, *ECMWF Newsletter* **No. 163**, 18–22.

Matthes, **K.**, **B. Funke**, **M. Anderson**, **L. Barnard**, **J. Beer**, **P. Charbonneau et al.**, 2017: Solar forcing for CMIP6 (v3. 2), *Geoscientific Model Development*, **10**, 2247–2302.

Moody, **E.G.**, **M.D. King**, **C.B. Schaaf**, **D.K. Hall** & **S. Platnick**, 2007: Northern Hemisphere five-year average (2000–2004) spectral albedos of surfaces in the presence of snow: Statistics computed from Terra MODIS land products, *Remote Sensing of Environment*, **111**, 337–345.

Polichtchouk, **I.**, **M. Diamantakis** & **F. Váňa**, 2020: Quintic vertical interpolation improves forecasts of the stratosphere, *ECMWF Newsletter* **No. 163**, 23–26.

Schaaf, **C.B.**, **F. Gao**, **A.H. Strahler**, **W. Lucht**, **X. Li**, **T. Tsang et al.**, 2002: First operational BRDF, albedo nadir reflectance products from MODIS. *Remote sensing of Environment*, **83**, 135–148.

A major moist physics upgrade for the IFS

Peter Bechtold, Richard Forbes, Irina Sandu, Simon Lang, Maike Ahlgrimm

After nearly five years of development, we are in the final stages of refinements and verification of major changes to the moist physics intended for implementation in the next upgrade of ECMWF's Integrated Forecasting System (IFS Cycle 48r1).

One of the main drivers of this project was ECMWF's strategic decision to move towards an ensemble forecast horizontal grid spacing of about 5 km, down from 18 km today. With this in mind, the project aimed to revise the moist physics to ensure that the complicated interactions between turbulence in the lowest part of the atmosphere, convective motions and the cloud physics are described as simply, efficiently, accurately and scale-independently as possible. These developments make it possible for the IFS to be run across a broader range of horizontal resolutions, including convection-permitting resolutions.

A second motivation for the moist physics upgrade was to tackle longstanding systematic model errors in clouds, precipitation and radiation across all resolutions and forecast lead times. Due to the sensitivity of the forecast to moist processes, the complex nature of atmospheric interactions, and compensating errors in the model, there is an increasing need to implement targeted combinations of physics changes together to address systematic errors in a more holistic way.

The upgrade brings a significantly improved physical basis for moist processes and is necessary to facilitate future development of the IFS. Here we give a short overview of changes in the representation of turbulence, clouds, and shallow and deep convection, with a focus on some of the main impacts of the upgrade. A more quantitative assessment of the impact of these changes on the overall performance of the forecasting system will be reported once IFS Cycle 48r1 has been implemented.

Parametrizing moist processes in the IFS

Moist processes in the IFS are represented with physically based parametrizations for turbulent mixing, convection, subgrid clouds and microphysics. Each parametrization is called sequentially during every model time step. Although parametrizations are often developed as separate entities, it is vital that they interact with each other in a physically consistent way to represent real-world processes effectively. There are therefore many dependencies between schemes. Individual developments over many years have led to some complications and inconsistencies in the way these schemes work together. For example, in the layer of the atmosphere most directly affected by surface heating and friction (the boundary layer), there are inconsistencies between the buoyant updraughts used in the turbulence and convection schemes. In addition, the separate cloud saturation adjustments in the turbulent mixing scheme often conflict with the main cloud scheme and there are multiple saturation adjustment steps throughout the timestep. These

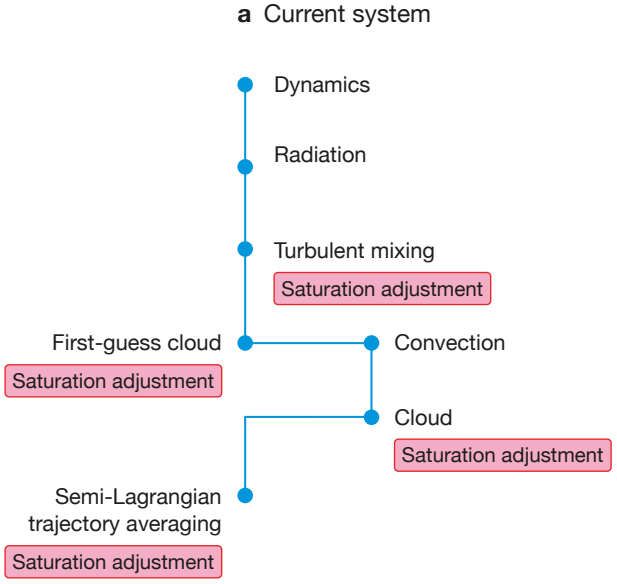

FIGURE 1 IFS physics parametrization call sequence, highlighting the differences in saturation adjustment between (a) moist physics in the current IFS and (b) the moist physics upgrade planned for IFS Cycle 48r1. In (a), half the temperature and humidity tendencies from the first-guess call to the cloud scheme are added to the state seen by the main convection and cloud schemes.

doi: 10.21957/3gt59vx1pb

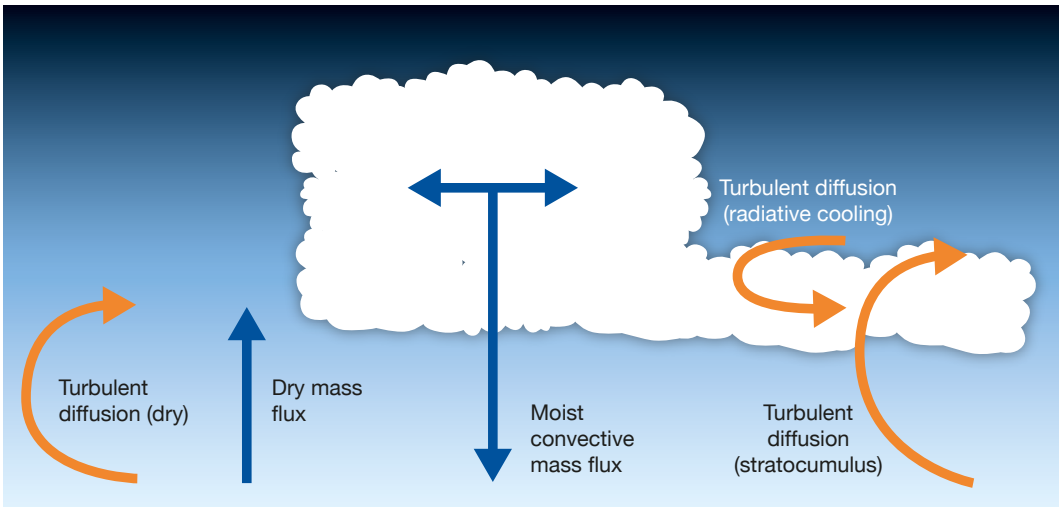

FIGURE 2 Schematic of the representation of the cloudy convective boundary layer in the IFS, consisting of moist convective mass flux in the moist convection scheme and dry mass flux and turbulent diffusion in the turbulence scheme. The turbulent diffusion coefficient K has a quasi-dry K-profile in a clear-sky boundary layer. In the presence of stratocumulus clouds, the K-profile Sc extends to the cloud top and contains an additional contribution from radiative cooling and cloud top entrainment.

inconsistencies have been resolved in the moist physics upgrade (Figure 1).

The convective boundary layer

In the IFS, the mixing in the convective boundary layer is represented by two schemes: a turbulence scheme (Köhler et al., 2011) and a moist convection scheme (Bechtold et al., 2014). The turbulence scheme comprises a turbulent eddy diffusion and mass flux scheme, which represents clear and stratocumulus-topped boundary layers. The moist convection scheme comprises a mass flux scheme for moist shallow and deep cumulus convection.

An important quantity in the turbulence scheme is the eddy diffusion coefficient K, which is computed using a K-profile closure. The scaling of the diffusion coefficients and the height to which diffusive mixing is applied depends on the mixed layer height. The latter is currently computed inside the turbulence scheme from a convective updraught model that is different from that used in the moist convection scheme. This convective updraught model is also used to diagnose if the boundary layer is clear or cloudy and to detect the cloud base. A distinction is made between a cumulus (Cu) and stratocumulus (Sc) topped boundary layer based on the inversion strength. For Sc cases, the moist convection scheme is switched off. The mixed layer height is equal to the boundary layer height for clear and Sc cases and to cloud base for Cu cases. Entrainment mixing is applied for all boundary layers, with an extra mixing term proportional to the radiative cooling at cloud top in Sc cases. The turbulent mass flux is only applied in clear boundary layers.

Clouds are represented by a separate cloud scheme (Tiedtke, 1993). In this scheme, detrainment from the moist convection scheme is an important source term. In addition, in an Sc-topped boundary layer, clouds are generated by a statistical subgrid condensation scheme that is embedded in the turbulent diffusion scheme.

The code structure and interactions between these three schemes has become complicated over time, leading to inconsistencies in physical assumptions. For example, the updraught model in the turbulence scheme estimates a much lower occurrence of Cu cases than the moist convection scheme. More importantly, there is no clear separation between processes, such as the dry and moist convective and turbulent mixing and the respective sources in the turbulence scheme on the one hand and the moist convection scheme on the other. We therefore decided to radically simplify the overall code structure and the turbulence scheme code in particular. The aim was to formulate consistent interactions between the schemes across all types of convective boundary layers, as indicated in the schematic in Figure 2.

The main scientific formulation of the physical processes for the convective boundary layer remains the same as before, but there are several important differences introduced with the moist physics upgrade:

- The mixed layer height up to which the K-profile is applied in the turbulence scheme is now computed using the same updraught model as that used in the moist convection scheme. The mixed layer height is still typically near the inversion top in the clear boundary layer, near the cloud base for Cu-topped boundary layers and near the cloud top for Sc-topped boundary layers.

- The criterion used to distinguish between Sc and Cu topped boundary layers has been revised by computing the strength of the temperature inversion using a new method, based on the variation of moist entropy (Marquet, 2010).
- At the top of the mixed layer, mixing via cloud top entrainment proportional to 20% of the surface buoyancy flux is applied for all types of boundary layers. In the case of Sc, an additional term is applied to represent radiatively driven entrainment. An increased contribution to turbulent mixing from radiative cooling is still applied in Sc-topped boundary layers.
- The shallow part of the moist convection scheme now does all the moist transport, including in stratocumulus, where it acts together with the radiatively driven turbulent mixing. This made it necessary to improve the numerical stability of the convection scheme as the divergence of the mass flux is large in Sc in the vicinity of inversions. The dry mass flux from the turbulence scheme is now applied only in clear boundary layers.
- The statistical cloud scheme has been removed from the turbulent diffusion scheme and all cloud processes are handled by the cloud scheme.
- The sub-time stepping (iteration) used for many years in the turbulence scheme has been removed, improving the computational efficiency of the IFS whilst maintaining the scheme's good performance.

The upgrade has improved the representation of turbulent and convective mixing in the convective boundary layer in a simple and consistent way that works for clear, cumulus- and stratocumulus-topped boundary layers and their transitions. Figure 3 shows an example of the transition from stratocumulus to cumulus along a section across the Pacific Ocean and highlights the more realistic behaviour of the modelled boundary layer cloud with the moist physics upgrade.

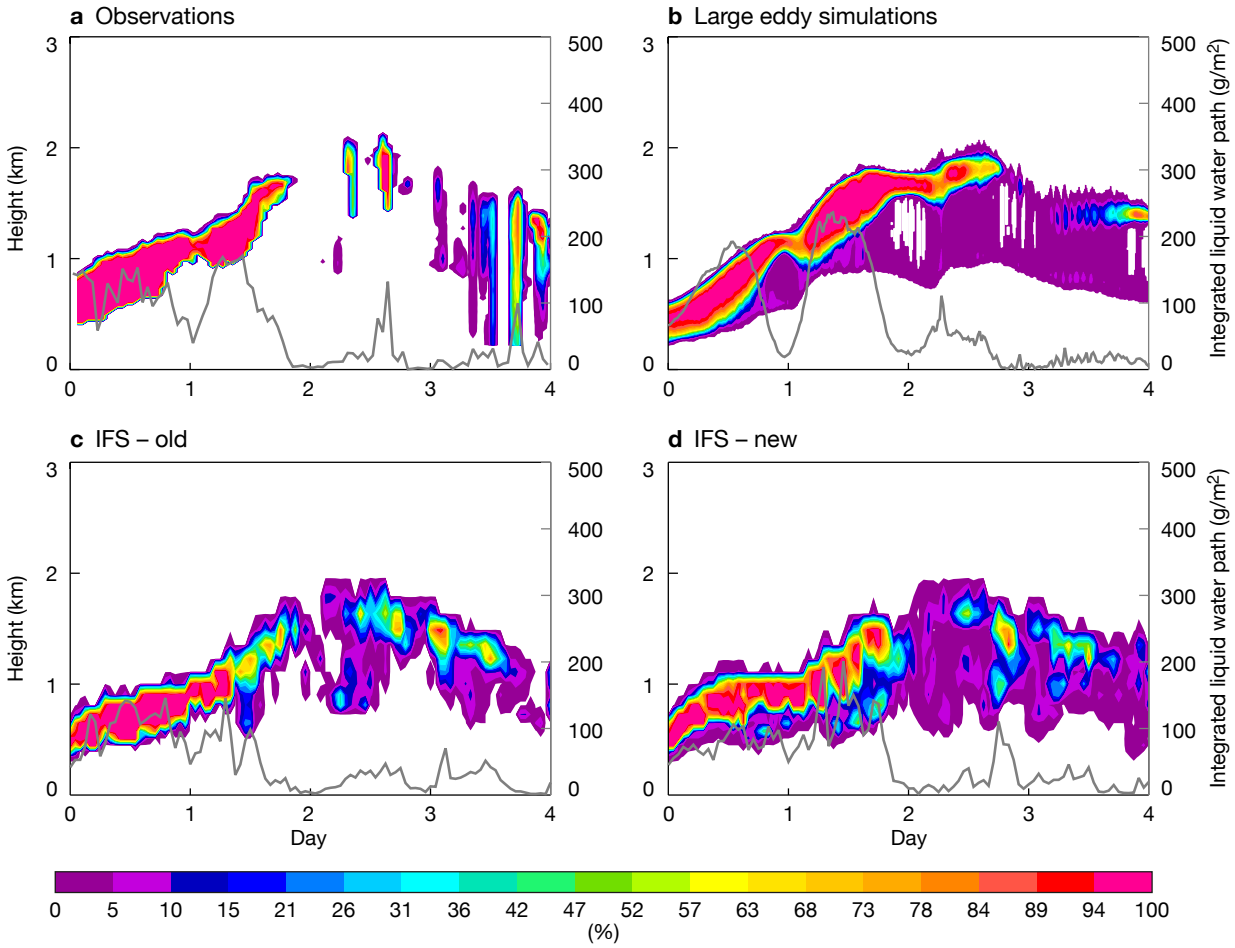

FIGURE 3 Cross section from the south Californian coast to Hawaii showing the evolution of cloud fraction profiles (shading) and integrated liquid water path (grey lines) from 21 to 25 July 2013 along the ship track of the Marine ARM GPCI Investigation of Clouds (MAGICS) campaign according to (a) instruments onboard the MAGICS ship, (b) large eddy simulations (LES) forced by IFS analyses, (c) re-forecasts starting at 00 UTC on 21 July using IFS Cycle 46r1 and (d) the same re-forecasts with the moist physics upgrade. Note that the radar in (a) has a sensitivity threshold and the plot shows a point profile, while (b), (c) and (d) show area means. This helps to explain the larger gaps in (a) compared to the other plots. The discrete steps in the rising cloud top in the IFS in (c) and (d) are due to the coarser vertical resolution compared to the LES.

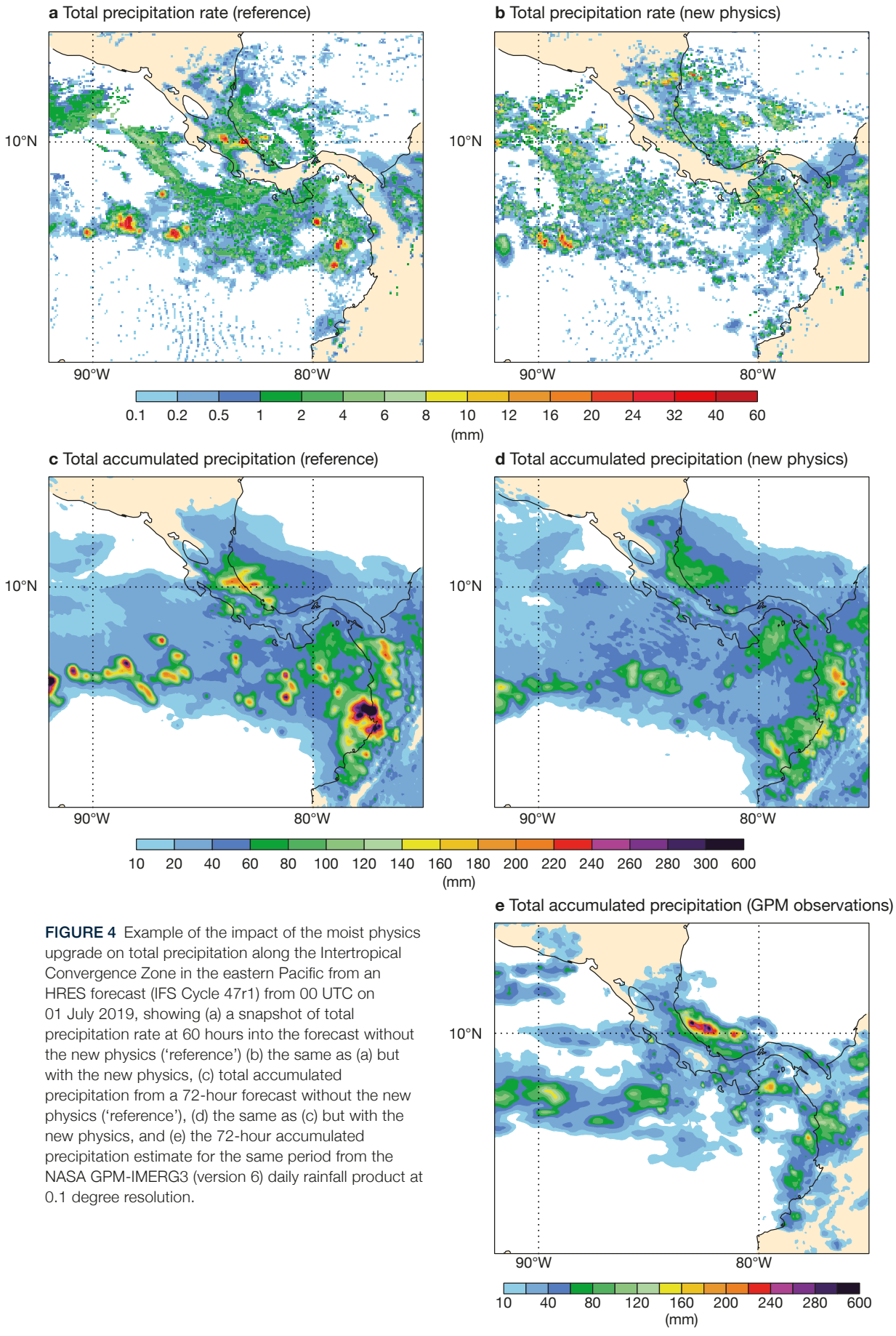

FIGURE 4 Example of the impact of the moist physics upgrade on total precipitation along the Intertropical Convergence Zone in the eastern Pacific from an HRES forecast (IFS Cycle 47r1) from 00 UTC on 01 July 2019, showing (a) a snapshot of total precipitation rate at 60 hours into the forecast without the new physics ('reference') (b) the same as (a) but with the new physics, (c) total accumulated precipitation from a 72-hour forecast without the new physics ('reference'), (d) the same as (c) but with the new physics, and (e) the 72-hour accumulated precipitation estimate for the same period from the NASA GPM-IMERG3 (version 6) daily rainfall product at 0.1 degree resolution.

Saturation adjustment and the cloud scheme

The saturation adjustment process calculates the amount of condensation or evaporation due to changes in temperature and humidity in a model grid box. It allows for partially cloudy grid boxes with subsaturation, and for supersaturation (with respect to ice) at temperatures below freezing in the clear air part of the grid box. The cloudy part is always at saturation (liquid or ice, depending on temperature).

The scheme assumes a simple form of subgrid variability of temperature and humidity to predict how the condensate and cloud fraction change due to various processes including adiabatic cooling, convective subsidence warming, turbulent mixing and microphysics. Saturation adjustment is performed in multiple places in the current IFS code with a different set of assumptions in the turbulence scheme compared to the rest of the model. Saturation adjustment in the IFS is therefore not straightforward and contains several assumptions, thresholds and limiters for numerical stability for long time steps, particularly for the ice phase. Several issues have been identified and are addressed as part of the moist physics upgrade:

- An overly complicated call sequence for cloud and convection processes was obscuring an error in the saturation adjustment to the temperature forcing from the dynamics. This has now been corrected as part of the moist physics upgrade. At the same time, the interactions between the turbulence, moist convection and cloud schemes have been significantly simplified so that saturation adjustment now only takes place in the cloud scheme (Figure 1). Positive impacts include a reduction in the number of overactive quasi-stationary precipitation cells, which have been a longstanding problem in the IFS in the tropics (Figure 4).
- The original saturation adjustment process in the IFS only modified cloud fraction in partially cloudy grid boxes as a result of changes in temperature. It included a separate step to adjust for supersaturation resulting from changes in humidity. This has been modified to take into account changes in temperature and humidity simultaneously. Doing so

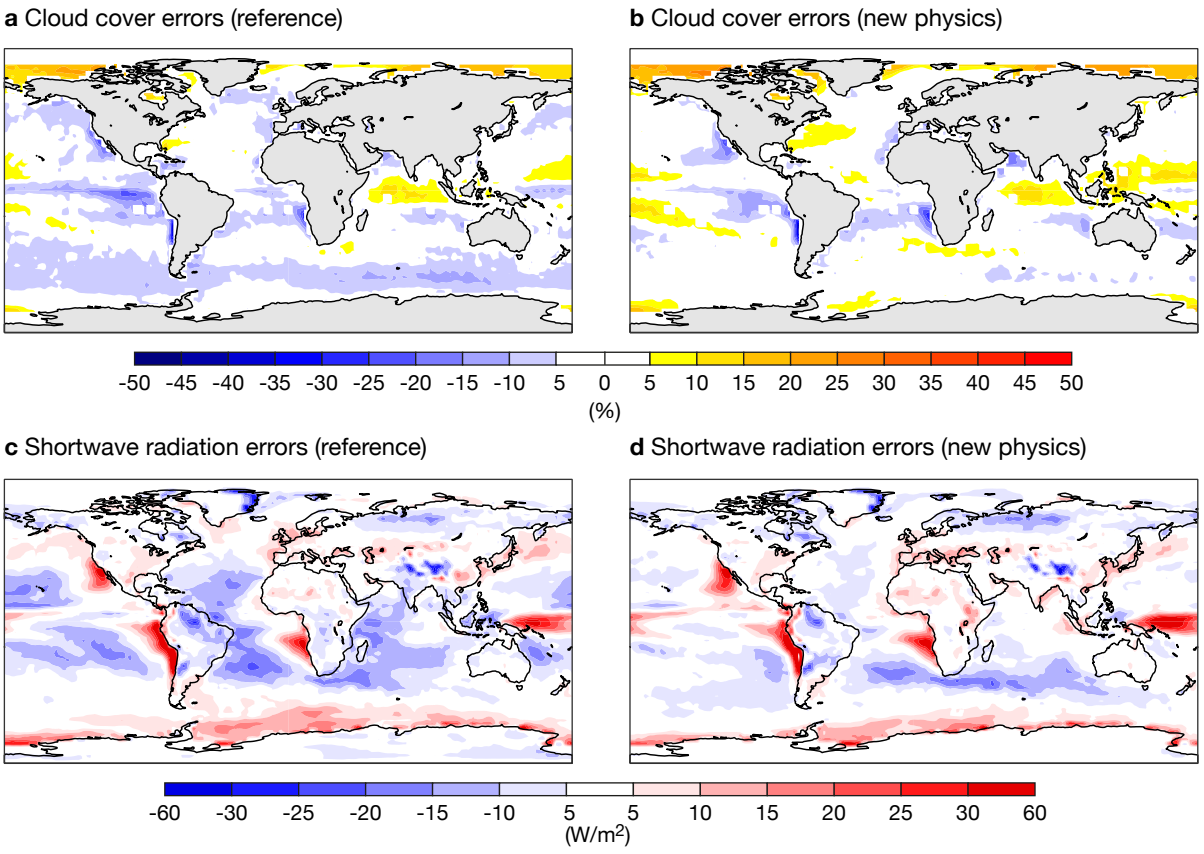

FIGURE 5 Cloud and radiation evaluation from a small ensemble of 1-year free-running coupled integrations with IFS Cycle 47r1. The charts show (a) the annual mean difference in total cloud cover over open water between the model and the Cloud-Aerosol Lidar and Infrared Pathfinder Satellite Observations (CALIPSO) climatology without the new physics ('reference'), (b) the same as (a) but with the new physics, (c) the annual mean difference in top-of-atmosphere net shortwave radiation between the model and the CERES–EBAF (Clouds and Earth's Radiant Energy System – Energy Balanced and Filled) product without the new physics ('reference') and (d) the same as (c) but with the new physics. Negative (positive) values correspond to excessive (insufficient) outgoing shortwave radiation. Longstanding systematic errors in cloud cover are reduced at the same time as improving the radiation fields.

enables direct input of tendencies from the moist convection and turbulence schemes. As mentioned earlier, the separate cloud scheme within the turbulence scheme has been removed, leading to a simpler and more consistent representation of cloud fraction tendencies across the model.

- For partially cloudy grid boxes, the threshold for maximum ice supersaturation in the clear-sky and the numerical limiter for condensation have both been revised to be more physically meaningful and consistent across processes. This beneficially increases the cloud cover in deep cloud systems and humidity in the mid-to-upper troposphere.
- In the current IFS, the slow physics tendencies are averaged along the semi-Lagrangian trajectory at the end of the time step. As this can introduce unphysical supersaturation due to inconsistencies in the averaged temperature and humidity, there is a final saturation adjustment step to remove any supersaturation. However, in practice this final adjustment step also removes a significant proportion of the supersaturation that should have been removed earlier by the cloud scheme. With the improved treatment of the saturation adjustment in the moist physics upgrade, these final tendencies now become small. This impacts the ensemble perturbations as more of the condensation warming due to the removal of supersaturation is done in the part of the tendencies that are included in the Stochastically Perturbed Parametrization Tendencies (SPPT) scheme. The result is a welcome increase in the spread of the ensemble in the first few days of the forecast.

Microphysical processes and interaction with radiation

The moist physics upgrade also improves the parametrization of microphysical processes by introducing additional processes for the depositional growth of precipitating snow, the evaporation of cloud ice, and the collision-collection of rain and snow particles. The warm-rain collision–coalescence process (autoconversion–accretion) at supercooled temperatures can now form supercooled rain drops. This will enable the IFS to predict the hazardous precipitation type ‘freezing drizzle’. This is different from the existing precipitation type ‘freezing rain’, which is produced through a different process.

Improving the realism of microphysical processes is an important part of reducing compensating errors and systematic errors in the model and improving forecast skill. Even small changes to processes such as the warm-rain formation process, rain evaporation or ice sedimentation can have significant impacts on the cloud and precipitation field and can affect shortwave and longwave radiation. To improve the realism of radiation further, the physics upgrade also includes a change to use the observed exponential–random vertical overlap of subgrid cloud fraction. ‘Exponential’ here refers to the exponential overlap within a cloud layer as a function of layer depth, and ‘random’ to the random overlap between separate cloud layers. This replaces the exponential–exponential cloud overlap scheme currently used in the IFS.

It is important to reduce systematic errors in the model, not only to reduce model bias for the assimilation system, but also for the longer range, as the predicted model state rapidly evolves away from the initial state towards the model’s own climate. The combined improvements to the turbulence, convection, cloud and radiation schemes affect many aspects of the forecast and help to reduce some significant systematic errors across forecast lead times. This is particularly true for cloud and its impacts on radiation (Ahlgrimm et al., 2018). As an example, Figure 5 shows how much the moist physics upgrade improves the model climate for global cloud cover and top-of-atmosphere shortwave radiation compared to observations. Although the lack of cloud in the subtropical marine stratocumulus regions has not yet been addressed, elsewhere both cloud and radiation errors have been significantly reduced in most places.

Deep convection and mesoscale convective systems

The moist physics upgrade also addresses errors in the parametrization of deep convection, especially for the representation of propagating mesoscale convective systems and their diurnal cycle. In particular, insufficient night-time convection over land has been identified as a major shortcoming in IFS forecasts of convective activity.

The issue is illustrated in Figure 6, which shows the evolution of convection on 12 August 2017 at 15, 18 and 21 UTC over Central Africa and the Sahel region. The plots show observations from the 10.8 μm infrared channel of Meteosat-10 (Figure 6a) and 3-hourly rain accumulations from the TRMM radar product 3B42 (Figure 6b). Consistently, these observations show mesoscale convective systems, including some in the band of 10–18°N that intensify during the afternoon and early night-time hours and propagate westward.

To explore the potential of the IFS to adequately represent such processes at future higher resolutions, we have rerun this case with IFS Cycle 46r1 but at 4 km horizontal resolution using the deep convection parametrization (Figure 6c) and without that parametrization (Figure 6d). As developed through a collaboration with Günther Zängl at the German national

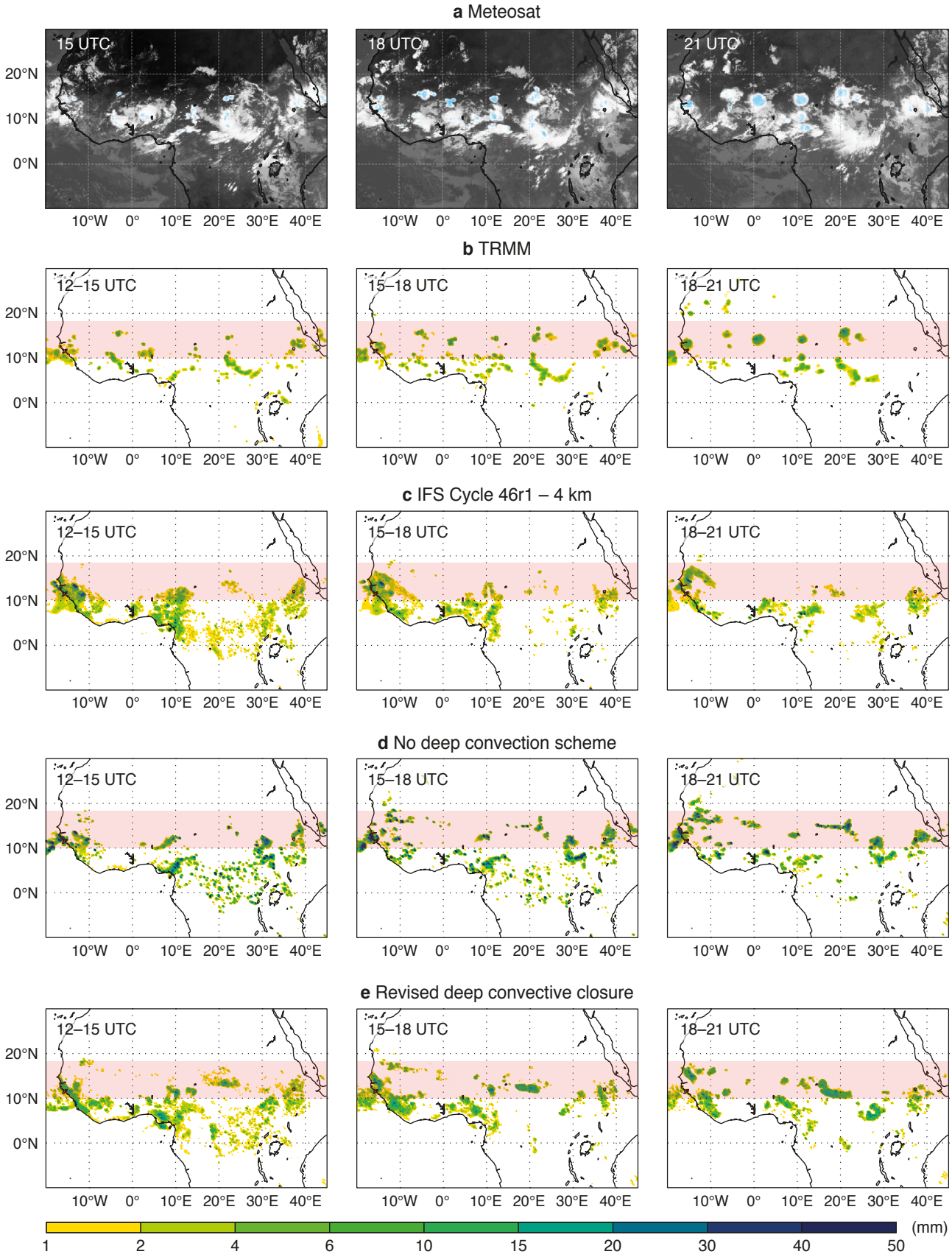

FIGURE 6 Evolution of continental convective systems over tropical Africa during 12 September 2017 as reflected in (a) Meteosat-11 infrared images at 10.9 μm wavelength at 15, 18 and 21 UTC, and (b) 3-hourly accumulated rainfall (mm) from 12–15, 15–18 and 18–21 UTC according to the TRMM 3B42 observational product. The other panels show the same as (b) but according to (c) 4 km re-forecasts using IFS Cycle 46r1, (d) 4 km IFS re-forecasts without the deep convection scheme, and (e) 4 km IFS re-forecasts with the revised deep convective closure. The IFS re-forecasts start at 00 UTC on 11 September 2017. There is no TRMM 3B42 data east of 29°E at 21 UTC. The evolution of precipitation in the highlighted band from 10–18°N is better reflected in (d) and (e) than in (c).

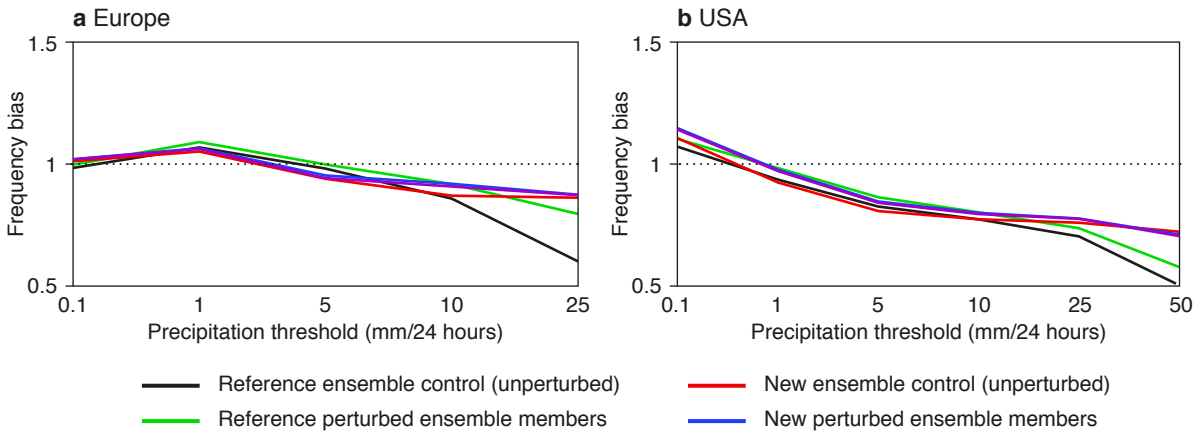

FIGURE 7 The plots show the frequency bias of 48–72-hour ensemble forecasts of total rainfall during June 2018 for different thresholds of precipitation compared to (a) OPERA radar observations over Europe and (b) NEXRAD-Stage IV radar data over the continental USA. Results are shown for one unperturbed member (Control) and the mean of eight perturbed members (Perturbed) using IFS Cycle 46r1 with and without the moist physics upgrade. The dotted line represents 'no bias'.

meteorological service (DWD), the deep convection parametrization includes a smooth reduction of the parametrized convective fluxes, and therefore a transition to resolved convection with increasing resolution (grid spacings smaller than 8 km).

With the deep convection parametrization, the rainfall patterns in Figure 6c are too broad-scale and the night-time propagating systems at 15°N are absent. Similar results are obtained with the operational 9 km grid spacing (not shown). In contrast, without the deep convection parametrization (Figure 6d) the representation of the intense westward-propagating mesoscale systems is improved. However, the amplitude of these systems is too strong, as is evident from a comparison with the TRMM data, and global precipitation is overestimated by more than 10%. Also, the root mean square error of precipitation and upper-air forecast skill are significantly degraded with this version of the model.

We have therefore decided to explore further avenues of improving the convection parametrization. These include the coupling between the convection and the dynamics, which is particularly delicate in the case of mesoscale convective systems that propagate and regenerate by producing their own horizontal convergence. During a research stay of Tobias Becker (Max Planck Institute for Meteorology) at ECMWF, we analysed output from runs without deep convection parametrization over Africa for the whole month of August. It was found that the lack of intense continental convection in the parametrization can be corrected for by including the total advective moisture convergence in the convective instability closure.
The results with the revised closure at 4 km are shown in Figure 6e. Using the revised parametrization makes the convection more intense than when using the current scheme, and realistic propagating features develop when compared with the observations in Figure 6b. Overall the results are now somewhere in between the current operational scheme and the simulations without the deep convection parametrization.

The evaluation of the IFS with the revised deep convection, which is part of the moist physics upgrade, is ongoing. The results so far have shown that the revised closure improves rainfall distribution and particularly the prediction of high rainfall rates.

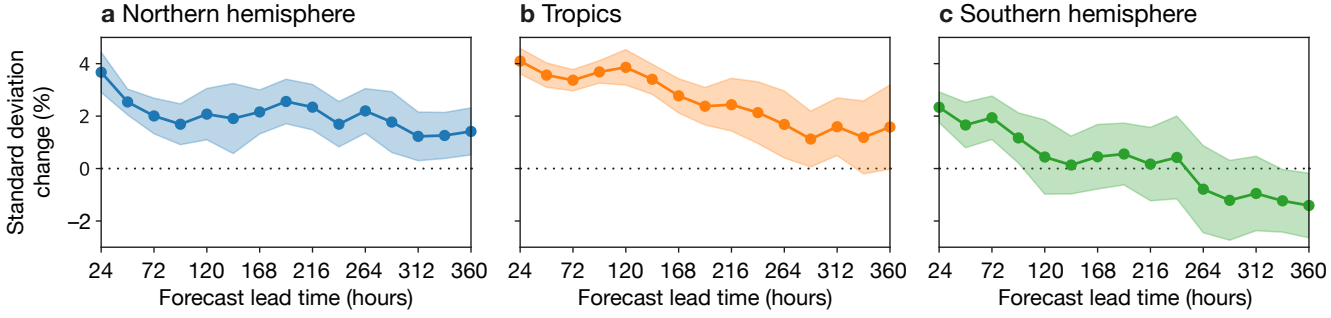

FIGURE 8 Relative change of 250 hPa wind speed ensemble standard deviation in a set of TCo399 ensemble forecasts using IFS Cycle 46r1 for June 2018 when the moist physics upgrade is applied, for (a) the northern hemisphere, (b) the tropics and (c) the southern hemisphere. The shaded areas show 95% confidence intervals.

It also improves the model variability in the medium and long range. However, it increases root-mean-square precipitation forecast errors by about 1–2% in short-range deterministic high-resolution forecasts. Figure 7 shows an evaluation of the frequency distribution of 48–72 h forecast rainfall totals against radar observations for June 2018 over Europe (OPERA data) and North America (NEXRAD-Stage IV data) using a small ensemble consisting of one unperturbed and eight perturbed members at resolution TCo399 (corresponding to a grid spacing of about 25 km). For both regions a clear underestimation of rainfall intensities >10 mm/24 h is evident in the operational model. The underestimation is alleviated by the revised closure.

Impact on ensemble forecasts

Testing of the ensemble system shows that the revised physics increases the activity of the model. For example, Figure 8 shows the relative increase of 250 hPa wind speed ensemble standard deviation (spread) compared to the IFS Cycle 46r1 baseline for June 2018. It is apparent that the ensemble spread is increased more strongly in regions where convection dominates perturbation growth, i.e. in the northern hemisphere (in summer) and in the tropics. Here, the spread increase persists out to day 15. This is valuable because the current operational ensemble forecasts are under-dispersive during the northern hemisphere summer for longer lead times. The increase in spread will make it possible to re-tune the stochastic model error representation.

Outlook

The moist physics package for IFS Cycle 48r1 is a major upgrade to the IFS which:

- addresses a number of long-standing issues in the formulation and interaction of parametrized convection, turbulent mixing and cloud-related processes
- improves the physical representation of the convective boundary layer, deep convection, cloud and precipitation in the forecast and
- reduces large-scale systematic errors in cloud and radiation.

There is also a beneficial increase in the activity of the forecast model and an improvement in the computational efficiency of the IFS by around 6%.

Final revisions and comprehensive testing of the physics upgrade across resolutions and timescales, from analysis increments to medium-range, extended-range and seasonal forecasts, will continue, in readiness for operational implementation. For the longer term, the upgrade is an important and vital step towards two strategic targets of ECMWF: ensemble forecasts at a horizontal grid spacing of about 5 km and a high-resolution ensemble where model uncertainty is represented by stochastically perturbed parametrizations (SPP; Leutbecher et al., 2017), in which parameter perturbations mainly stem from the model physics.

Concerning the future evolution of the moist physics parametrizations, we are currently testing the turbulent kinetic energy scheme developed by Météo-France. Further development of the subgrid cloud scheme and microphysics is planned in readiness for convection-permitting resolutions. Our good collaboration with the German national meteorological service (DWD) on the convection scheme continues as we have a joint implementation in the DWD's ICON model and the IFS. Furthermore, Météo-France is preparing to adapt and implement the deep convection code in its Arpège model Cy46T1.

Further reading

Ahlgrimm, **M.**, **R.M. Forbes**, **R.J. Hogan** & **I. Sandu**, 2018: Understanding global model systematic shortwave radiation errors in subtropical marine boundary layer cloud regimes. *J. Adv. Model. Earth Syst.*, **10**, 2042–2060.

Bechtold, **P.**, **N. Semane**, **P. Lopez**, **J.-P. Chaboureau**, **A. Beljaars** & **N. Bormann**, 2014: Representing equilibrium and non-equilibrium convection in large-scale models. *J. Atmos. Sci.*, **71**, 734–753.

Köhler, **M.**, **M. Ahlgrimm** & **A. Beljaars**, 2011: Unified treatment of dry convective and stratocumulus-topped boundary layers in the ECMWF model. *Q. J. R. Meteorol. Soc.*, **137**, 43–57.

Leutbecher, **M.**, **S.-J. Lock**, **P. Ollinaho**, **S.T.K. Lang**, **G. Balsamo**, **P. Bechtold et al.**, 2017: Stochastic representations of model uncertainties at ECMWF: state of the art and future vision. *Q. J. R. Meteorol. Soc.*, **143**, 2315–2339, doi:10.1002/qj.3094.

Marquet, **P.**, 2010: Definition of a moist entropy potential temperature: application to FIRE-I data flights. *Q. J. R. Meteorol. Soc.*, **137**, 768–791.

Tiedtke, **M.**, 1993: Representation of clouds in large-scale models. *Mon. Wea. Rev.*, **121**, 3040–3061.

Enhancing tropical cyclone wind forecasts

Jean-Raymond Bidlot, Fernando Prates, Roberto Ribas, Anna Mueller-Quintino, Marijana Crepulja, Frédéric Vitart

This article highlights two developments that have enhanced the usefulness of tropical cyclone wind forecasts in ECMWF's newly upgraded Integrated Forecasting System (IFS Cycle 47r1). The first is a change in the model specification for momentum exchange at the sea surface. This development is the result of internal ECMWF work informed by discussions with scientists at Météo-France and the US National Centers for Environmental Prediction (NCEP). It goes some way towards resolving the longstanding issue that predicted tropical cyclone maximum surface wind speeds are generally too low, in particular for intense tropical cyclones. The second development is the production of new forecast parameters which specify the maximum distance from the centre of the cyclone to locations where the surface wind speed reaches 34, 50 and 64 knots (wind radii). This will help users to assess the risk of wind-related hazards.

The maximum wind speed problem

Both minimum central pressure and maximum 10 m wind speeds are used as measures of tropical cyclone (TC) intensity. There have been several improvements recently in predicting minimum central pressure and overall cyclone tracks (Haiden et al., 2019). However, prior to IFS Cycle 47r1, ECMWF forecasts generally severely underestimated maximum wind speed for intense tropical cyclones even given the correct central pressure (Figure 1a). While there are many different factors that could account for this behaviour, we have found it to be closely linked to the parametrization of momentum exchange at the ocean surface.

This momentum exchange is generally expressed in terms of the drag coefficient (Cd), which connects the magnitude of the surface stress to the square of the wind speed at a certain height above the surface. In the IFS, there is an active two-way coupling between the atmosphere and ocean waves, which results in an extra

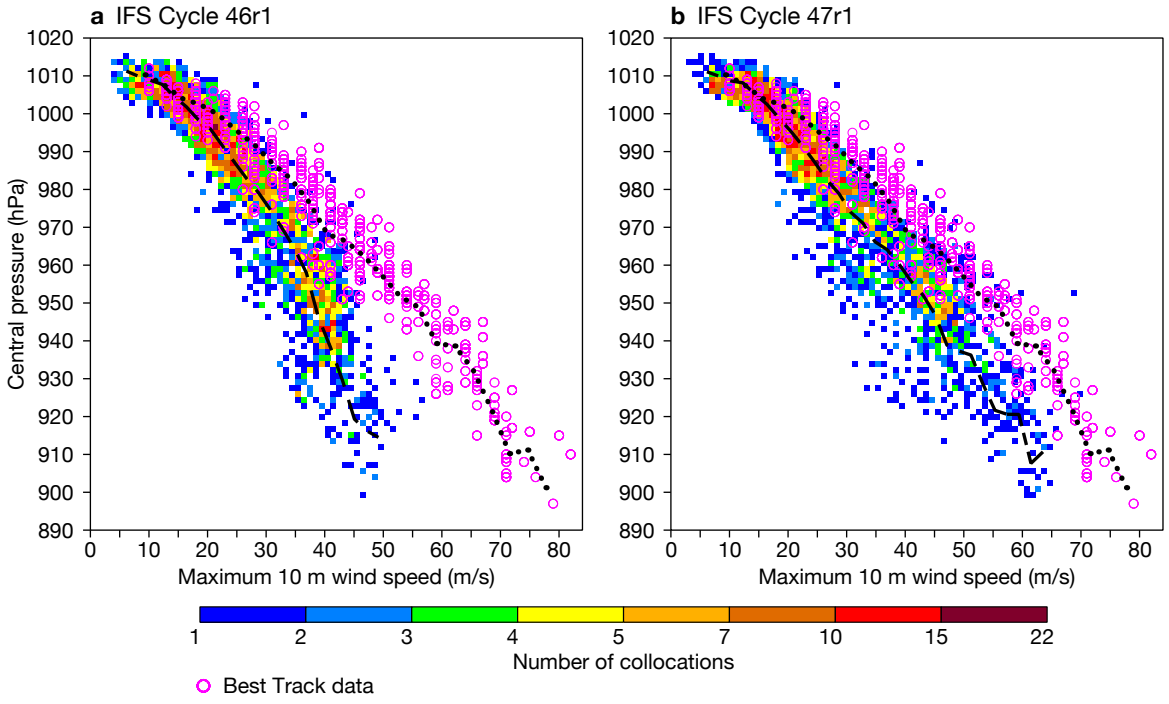

FIGURE 1 Scatter plots for maximum 10 m wind speed and corresponding minimum mean sea level pressure for all 10-day forecasts at TCo1279 resolution (corresponding to a grid spacing of about 9 km) from 00 UTC for the period 25 August 2019 to 1 January 2020 (coloured squares; the dashed line indicates mean central pressure for a given wind speed), and corresponding reported values (6-hourly Best Track data; purple circles; the dotted line indicates mean central pressure for a given wind speed), for 20 tropical cyclones, showing results for (a) IFS Cycle 46r1 and (b) IFS Cycle 47r1 with the new parametrization of unresolved roughness.

doi: 10.21957/k0w4fp581h

dependency of Cd on the sea state (waves). Figure 2a shows the distribution of Cd values in IFS Cycle 46r1 plotted against wind speed for Hurricane Irma in September 2017. There is a large spread of possible Cd values for most wind speeds, in part due to the sea-state effect, with a tendency for the drag coefficient to take larger values for stronger winds.

Over the last decade, it has been suggested that the drag coefficient should tail off for strong winds. Recent wave model developments have tried to address this issue. Since IFS Cycle 43r1 (November 2016), maximum wave spectral steepness criteria have been imposed on the evolution of the wave spectra, resulting in reduced Cd values for high winds (Magnusson et al., 2019). Moreover, with the introduction in IFS Cycle 46r1 of a new parametrization of wind input and whitecap dissipation (June 2019), a further reduction of large Cd values, with a slight decrease for high winds, was achieved. However, a mismatch between predicted and observed maximum winds persisted, and a recent paper by Donelan (2018) indicated that the drag coefficient should decrease quite significantly for hurricane-force winds.

Improving maximum winds

In the IFS, the momentum exchange with the sea surface is modelled via a dependency of the roughness length (z_0) on the surface stress. This expression accounts for both low and high wind regimes. At low wind speed, the sea surface becomes aerodynamically smooth and z_0 is determined by viscosity. At high wind speed, Charnock's relation is used, in which z_0 is expressed as a function of surface stress, air density, gravitational acceleration and a sea-state-dependent Charnock parameter. In ECMWF's wave model, the Charnock parameter depends on the state of development of the resolved waves and a tuneable parameter (α_b) which represents the impact of unresolved short waves (background roughness beyond the highest frequency resolved by the model) on the overall surface stress. Until IFS Cycle 47r1, this parameter had a constant value.

Observational evidence that the drag coefficient should be much lower for high winds suggests that the coupling between the ocean surface and the wind above becomes less efficient at transferring momentum for strong winds. For this to happen, it was realised that the Charnock parameter should be considerably smaller in the case of strong winds (above 35 m/s). This was achieved by reducing α_b for high 10 m wind speeds.

This simple reduction was implemented in IFS Cycle 47r1. As expected, the drag coefficient is sharply reduced for winds above 35 m/s. Figure 2 illustrates how this affects the frequency of high winds in tropical cyclone forecasts. In particular, it can be seen that there are many more instances of very high winds, up to about 70 m/s, than without the reduction in α_b.

The results shown in Figure 2 were obtained for forecasts at the experimental resolution of TCo1999 (corresponding to a horizontal grid spacing of about 5 km) in order to test the limit of this new parametrization. For the current

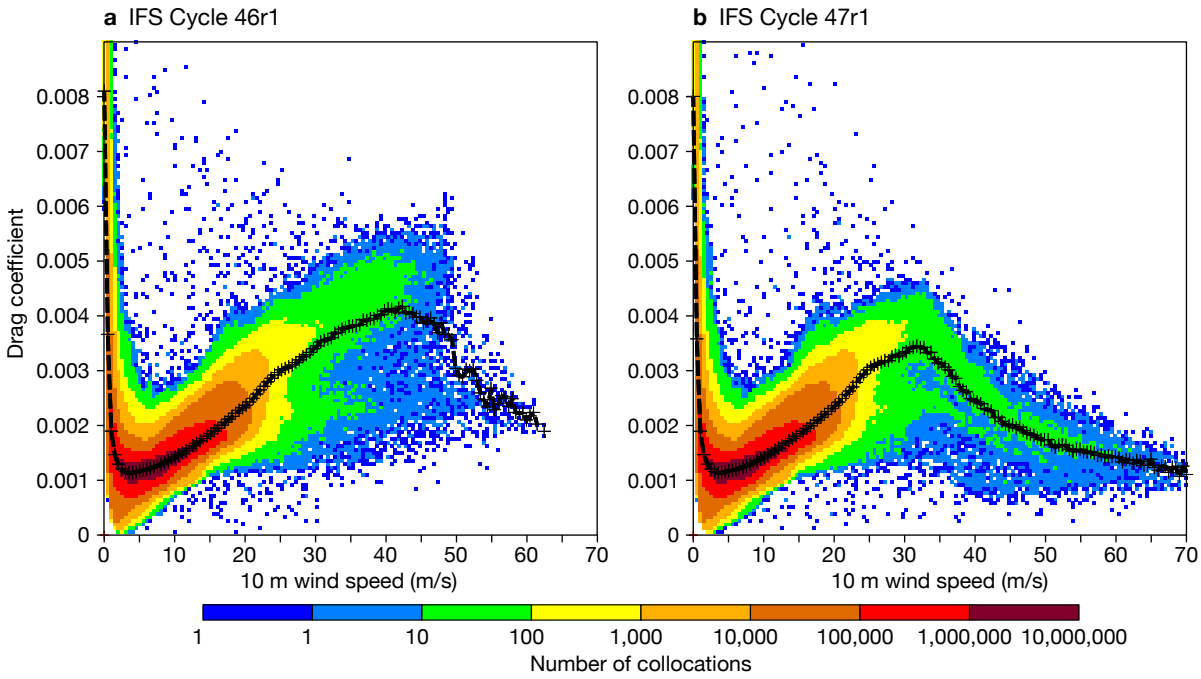

FIGURE 2 Scatter plots for the drag coefficient and corresponding 10 m wind speed for TCo1999 10-day forecasts initialised from the operational analysis of 00 UTC on 4 September 2017 (during Hurricane Irma), showing results for (a) IFS Cycle 46r1 and (b) IFS Cycle 47r1 with the new parametrization of unresolved roughness. All model grid points over the oceans were used every 6 hours. The black crosses show mean Cd values for given wind speeds.

operational resolution (TCo1279, about 9 km), we have looked at a range of tropical cyclone forecasts and found that, generally, the new parametrization yields a much better maximum wind speed – minimum pressure relation (Figure 1b). However, compared to observational estimates, forecasts continue to underestimate some of the most intense cases.

Computation of wind radii

To assess wind-related hazards associated with tropical cyclones, it is useful to see the areas where winds are predicted to exceed certain thresholds. In IFS Cycle 47r1, this has been made possible by introducing a new wind radii parameter. The parameter indicates the maximum distance from a TC centre within which the surface wind speed is predicted to exceed certain thresholds. The thresholds have been set at 34, 50 and 64 knots, in line with the values used by global tropical cyclone warning centres. To compute the wind radii, a specific module taken from the Vortex Tracker package (Biswas et. al., 2018) developed at the Geophysics Fluid Dynamics Laboratory (GFDL) is used. It was chosen for two main reasons: first, the GFDL Tracker has been extensively tested by research and operational communities; second, the GFDL and ECMWF trackers use the same programming language, which facilitated porting the module into the ECMWF operational system.

The wind radii computation is performed after the ECMWF TC tracker has completed the identification of cyclonic features for both high-resolution forecasts (HRES) and ensemble forecasts (ENS). It is carried out for all TCs that are present from analysis time and also those that develop during the forecast. To start, the algorithm establishes four sectors (NE, SE, SW and NW quadrants) centred on each TC's predicted positions. Within these sectors, the only model grid points considered are those whose distance from the TC centre is shorter than a predetermined radius, this radius being the distance beyond which winds are ordinarily below 34 knots. In each sector the distances of those grid points from the TC centre are then ranked, and 10 m wind speeds are checked at each grid point against the 34-, 50- and 64-knot thresholds. The wind radii then represent, for each sector, the maximum extent from the storm centre at which those wind thresholds are exceeded.

If the distance of a point where the wind speed is at least 34 knots is very close to the initial predetermined radius, then an iterative process follows: the predetermined radius is increased slightly and the scheme starts again until a more accurate 34-knot wind radius is reached. This iterative process is important to deal with situations where the storm is large and 34-knot winds are spread out far from the TC centre.

Finally, the upgrade to IFS Cycle 47r1 was an opportune time to remove the ad hoc factor converting 10-minute wind speeds to pseudo 1-minute wind speeds in the output files of the TC tracker (i.e. wind speed in m/s was multiplied by 2.1 to convert into knots until IFS Cycle 46r1, instead of using the standard conversion factor of 1.9). Historically, when models had very coarse horizontal resolutions and consequently TCs were too weak in forecasts, this conversion factor provided more realistic values. However, substantial progress made in recent years (including several model resolution upgrades) has improved the accuracy of TC forecasts, and tests confirmed that it could be removed without reducing forecast quality. Users should not expect an overall reduction in 10 m winds due to the removal of the ad hoc factor. On the contrary, 10 m wind speeds should be higher, at least for hurricane-force winds. Direct model output 10 m wind forecasts are not affected by removing the ad hoc factor.

Forecasting the size of Hurricane Dorian

Figure 3 shows an example of an HRES wind radii forecast starting from 12 UTC on 30 August 2019. Storm Dorian, which formed in the Atlantic basin on 24 August 2019, was elevated to hurricane category on 28 August while passing east of the island of Puerto Rico. Two days later, Dorian became a major hurricane before moving towards the Bahamas. The HRES 34-knot wind radii forecast is represented by circle sectors for each quadrant in 12-hour time steps. It means that 34-knot winds are predicted anywhere within those sectors. Similar charts are available for 50- and 64-knot wind radii if such wind speeds are present in the forecast.

Time series of the wind radii forecasts from the HRES can be compared with observation-based information (a combination of satellite passive microwave data, surface observations, and reconnaissance aircraft when available). Figure 4 shows the evolution of mean wind radii over all four quadrants based on a method using infrared satellite imagery (Knaff et al., 2016) and the HRES mean wind radii forecast for Hurricane Dorian from the same start date as before. Overall the model tends to underestimate the size of the wind structure around Hurricane Dorian for all wind thresholds. This suggests a problem in handling a medium-size system experiencing rapid intensification. As predicted by the forecast (Figure 3), Hurricane Dorian never made landfall in the Florida peninsula. We recommend using the wind radii from the ENS in order to quantify the risk of wind-related impacts, in particular in the medium range. Users are also advised to always combine TC track forecasts with the wind radii forecasts.

Verifying wind radii forecasts is difficult due to the lack of surface wind observations, which are critical for obtaining an accurate wind structure of the storms (Cangialosi & Landsea, 2016). This is why TC forecasting centres are still reluctant to publicly release on a regular basis

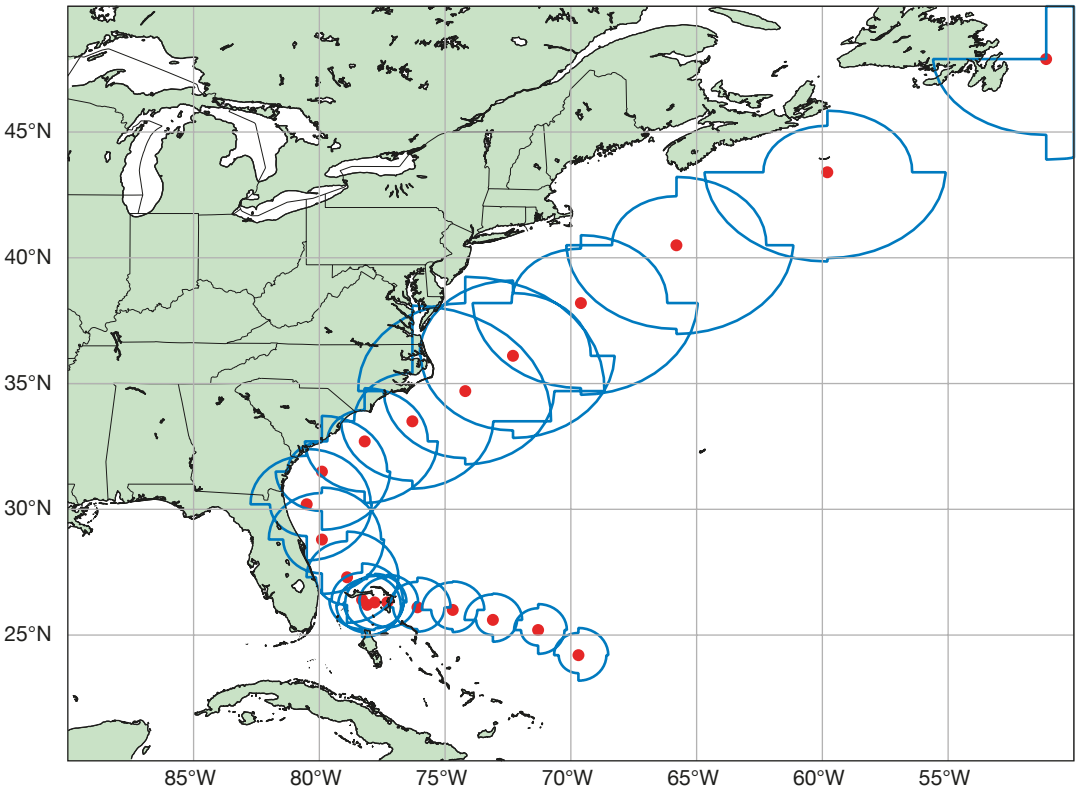

FIGURE 3 HRES wind radii forecast (IFS Cycle 47r1) for the 34-knot wind threshold up to 240 hours ahead, initialised at 12 UTC on 30 August 2019. The red dots indicate the predicted centre of Hurricane Dorian at 12-hour intervals.

verification metrics of TC size forecast performance. Despite these limitations, we have performed systematic verification for the northern hemisphere using the International Best Track Archive for Climate Stewardship (IBTrACS) dataset. Figure 5 shows the systematic errors of wind radii for the 34-, 50- and 64-knot wind speed thresholds of the HRES based on experiments carried out using IFS Cycle 47r1. Verification of ENS wind radii will be carried out once a sufficiently large sample is available. The HRES results suggest a tendency to underestimate the wind structure of TCs for all forecast lead times (consistent with the example of Hurricane Dorian shown in Figure 4). The systematic biases (mean errors) vary little with lead time except for the radius bias for the 34-knot wind speed threshold. Absolute wind radii errors are similar for 34- and 50-knot winds and nearly twice as big as the errors for the 64-knot wind speed threshold.

Product availability

To disseminate the wind radii product, changes had to be made in the publicly available tropical cyclone track BUFR files to accommodate this supplementary data. Three additional data descriptors were included in the BUFR messages: 'wind speed threshold', 'bearing/azimuth' and 'maximum radius for a given wind threshold'. To decode the TC product files, users will need a specific version of ecCodes or they can download the BUFR table version 33 of the BUFRDC.

More information can be found on this web page: *https://confluence.ecmwf.int/display/FCST/New+Tropical+Cyclone+Wind+Radii+product*.

Outlook

Progress has been made in improving the relationship between predicted maximum wind speed and predicted minimum mean sea level pressure for intense TCs. This has been achieved by introducing a change to the parametrization for the momentum transfer in IFS Cycle 47r1. The current approach relies on reducing the Charnock parameter when the 10 m wind is above a threshold value. Ongoing research aims to revise the parametrization based on an improved representation of the impact of ocean waves on high winds.

In addition, a new metric providing information on the surface wind speed structure and thus the size of a TC for the HRES and ENS is now available to users. It opens the way to adding other TC structure metrics in the future, in line with the recommendations of the World Meteorological Organization working group on tropical cyclones. Doing so will support forecasting centres and it will also provide additional metrics for model verification.

These two developments are expected to help forecasting centres around the world to provide better warnings of hazards related to high-impact TCs.

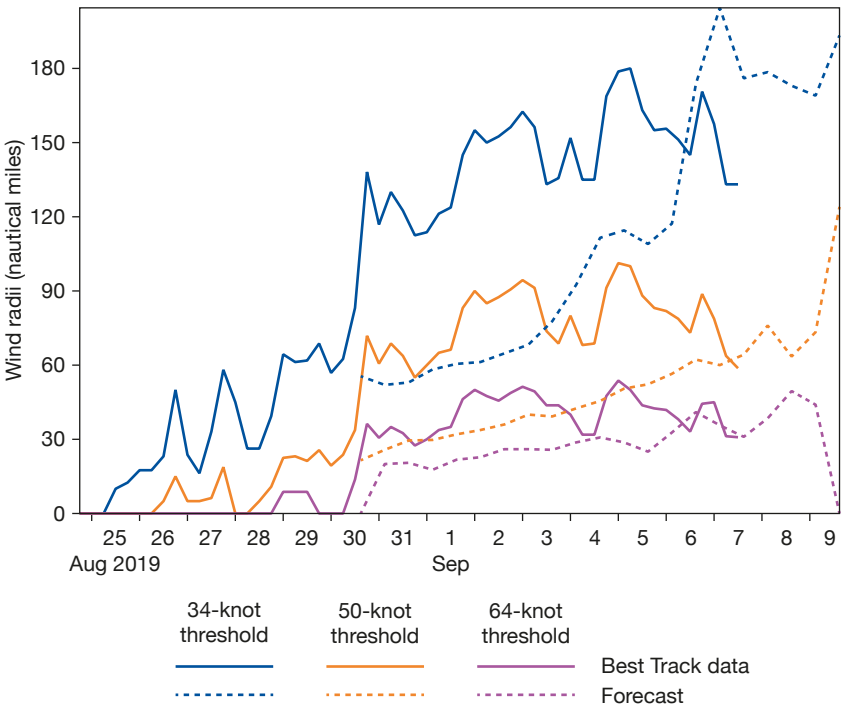

FIGURE 4 Mean HRES wind radii forecasts (dotted lines) for the 34-, 50- and 64-knot wind thresholds produced using IFS Cycle 47r1 and initialised at 12 UTC on 30 August 2019, and Best Track data (solid lines) for Hurricane Dorian.

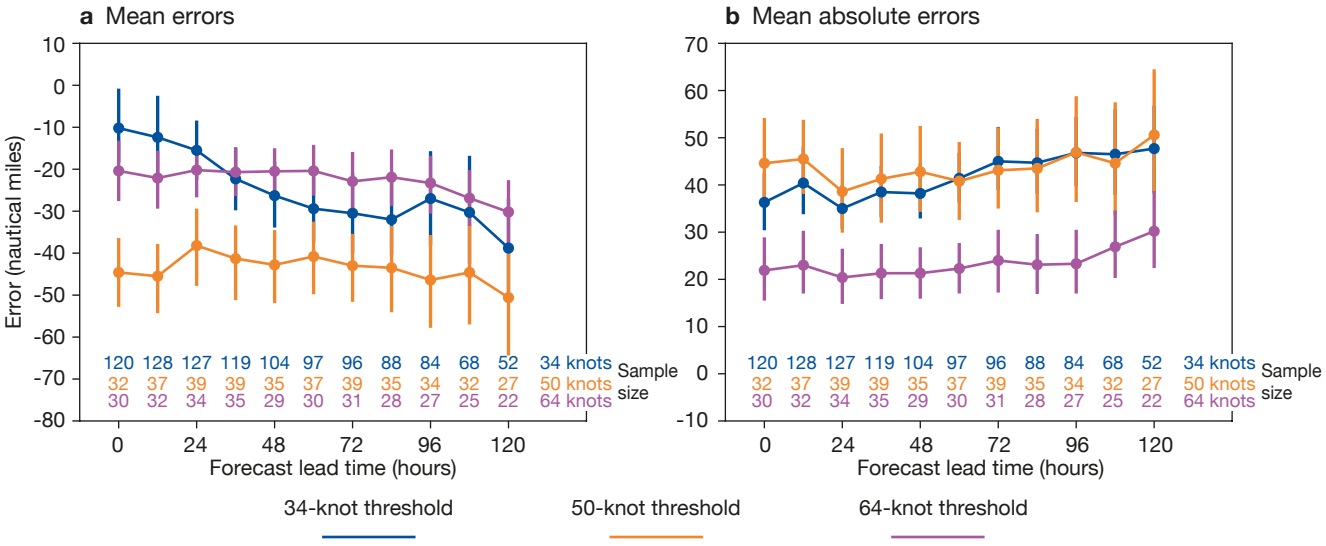

FIGURE 5 The charts show (a) the mean error of mean wind radii forecasts for 34-, 50- and 64-knot thresholds compared to Best Track data as a function of lead time up to 120 hours ahead and (b) the same but for mean absolute errors. Sample size is indicated at the bottom of the plot. The results were obtained for the TC basins in the North Atlantic and the Eastern Pacific (extended to the Western Pacific only for the 34-knot wind speed threshold) between July and November 2019. The vertical bars show 95% confidence intervals.

Further reading

Biswas, **M.K.**, **D. Stark** & **L. Carson**, 2018: GFDL Vortex Tracker Users' Guide V3.9a.

Cangialosi, **J. P.** & **C.W. Landsea**, 2016: An examination of Model and Official National Hurricane Center Tropical Cyclone Size Forecasts. *Weather and Forecasting*, **31**, 1293–1300.

Donelan, **M.A.**, 2018. On the decrease of the oceanic drag coefficient in high winds. *J. Geophys. Res.*, **123**, 1485–1501, doi.:10.1002/2017JC013394.

Haiden, **T.**, **M. Janousek**, **F. Vitart**, **L. Ferranti** & **F. Prates**, 2019: Evaluation of ECMWF forecasts, including the 2019 upgrade. *ECMWF Technical Memorandum* **No. 853**.

Knaff, **J.A.**, **C.J. Slocum**, **K.D. Musgrave**, **C.R. Sampson** & **B.R. Strahl**, 2016: Using routinely available information to estimate tropical cyclone wind structure. *Mon. Wea. Rev.*, **144**, 1233–1247.

Magnusson, **L.**, **J.-R. Bidlot**, **M. Bonavita**, **A. Brown**, **P. Browne**, **G. De Chiara et al.**, 2019: ECMWF activities for improved hurricane forecasts. *Bulletin of the American Meteorological Society*, **100**, 445–458, doi.:10.1175/BAMSD180044.1.

From weather forecasting to climate modelling using OpenIFS

Joakim Kjellsson (GEOMAR and University of Kiel, Germany), Jan Streffing (AWI, Germany), Glenn Carver, Marcus Köhler (both ECMWF)

Current activities at the GEOMAR Helmholtz Centre for Ocean Research in Kiel and the Alfred Wegener Institute, Helmholtz Centre for Polar and Marine Research (AWI) in Bremerhaven, Germany, include developing two new versions of high-resolution coupled climate models. Both climate models successfully use OpenIFS, a portable version of ECMWF's Integrated Forecasting System (IFS) for use at universities and research institutes.
The experience gained in using OpenIFS for climate modelling can in turn provide insights that will help ECMWF to further develop the IFS.

Benefits of using OpenIFS

It is becoming increasingly clear that high horizontal resolution can be very beneficial for coupled climate models. Experiments with the ECMWF forecasting system and as part of the high-resolution climate model intercomparison project, HighResMIP, have shown that increasing the horizontal resolution in a coupled climate model reduces biases, improves the representation of air–sea interactions, and enhances predictability. In addition, increased horizontal resolution in the atmospheric model can improve orographic drag, which in turn can reduce biases in the jet stream position, blocking and storm tracks.

GEOMAR and AWI are both known for developing and running eddy-rich ocean-only models with high horizontal resolution using grid refinement. At AWI, the FESOM2 ocean model employs an unstructured mesh, where the horizontal resolution is spatially variable depending on, for example, sea-surface height variance, local Rossby radius etc. At GEOMAR, the NEMO ocean model uses a grid refinement tool, AGRIF, to refine the mesh in specific basins, e.g. the North Atlantic or the South Atlantic/Western Indian Ocean. Both institutes have built coupled climate models using their respective eddy-rich ocean models coupled to the ECHAM6 atmospheric model: FOCI at GEOMAR (Matthes et al., 2020) and AWI-CM at AWI (Sidorenko et al., 2015). These coupled models will be used in a variety of projects in the future. However, ECHAM is no longer actively developed and has poor computational efficiency when running at higher horizontal resolutions than ~0.5°. The institutes have therefore developed new versions of FOCI and AWI-CM which use the ECMWF OpenIFS atmospheric model (Figure 1). This comes with a number of benefits.

First, the OpenIFS model is well suited to run at both low and high horizontal resolutions. As an example, a simulation with ECHAM6 with 95 vertical levels and a horizontal resolution of 1.875° (209 km grid spacing at the equator) running on 600 cores runs at about the same speed as OpenIFS (IFS Cycle 40r1) with 91 vertical levels and a horizontal resolution of 1.125° (125 km) on 280 cores, i.e. OpenIFS runs at less than half the computational cost at higher spectral and grid-point resolutions. The ability to run OpenIFS at higher atmospheric resolutions therefore enables scientists at GEOMAR and AWI to make full use of their high-resolution

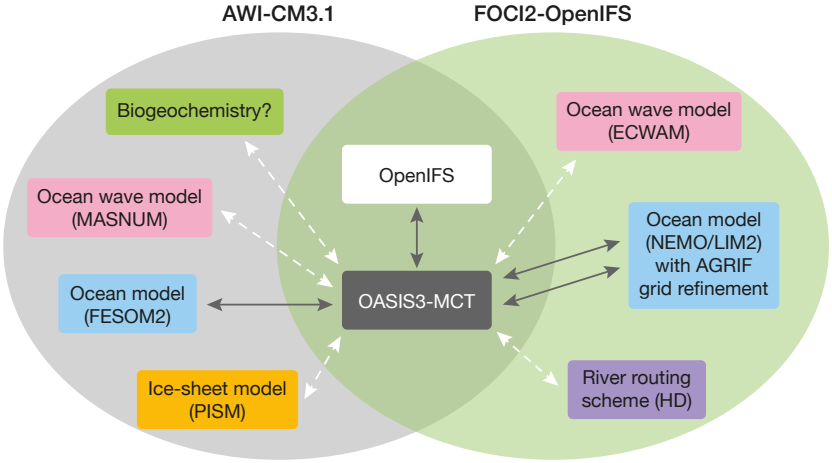

FIGURE 1 Schematic of the AWI-CM3.1 (grey circle) and FOCI2-OpenIFS (green circle) coupled climate models from AWI and GEOMAR, respectively. Both use the OpenIFS atmospheric model and the OASIS3-MCT coupler. Dark lines show couplings to components currently in use, while light dashed lines show couplings planned for future versions. Note that AGRIF is embedded within the NEMO executable but has its own coupling to OASIS3-MCT.

doi: 10.21957/469hc10jk5

ocean models in the coupled climate models they run.

Second, the OpenIFS model has an active and growing user community and a small support team at ECMWF who are able to assist when configuring atmosphere-only and coupled simulations.

Third, the OpenIFS model includes much of the world-leading science provided by ECMWF's IFS in a portable atmosphere–land–wave model. The addition of interfaces to the OASIS coupler allows it to be integrated into existing modelling frameworks.

Fourth, joining the OpenIFS community strengthens the collaborations between AWI, GEOMAR, the EC-Earth consortium and ECMWF, which has proven beneficial for all parties.

OpenIFS for climate modelling

The IFS has already been used for climate modelling purposes both as part of the EC-Earth model and by ECMWF scientists for the EU-funded PRIMAVERA project (Roberts et al., 2018), while the closely related ARPEGE-Climat is used in the French National Centre for Meteorological Research (CNRM) climate model (Table 1). Now AWI and GEOMAR have jointly adapted the OpenIFS model for climate integrations with contributions from the EC-Earth community. In addition, the EC-Earth model version 4 will also use OpenIFS, although this is very much at a prototype stage.
The modifications to OpenIFS by AWI and GEOMAR include adding interfaces for the OASIS3-MCT coupler; a river-routing scheme; and forcings from the World Climate Research Programme's Coupled Model Intercomparison Project (CMIP5 and CMIP6) as well as orbital forcing parameters for paleoclimate simulations. The OASIS development team contributed to the development of the OASIS interfaces in the OpenIFS model with dedicated support from the EU-funded IS-ENES3 (Infrastructure for the European Network for Earth System Modelling) project.

The AWI and GEOMAR models with OpenIFS – AWI-CM3.1 and FOCI2-OpenIFS respectively – use the same workflow manager, ESM-Tools (Barbi et al., 2020), to manage the simulations, e.g. compiling the model, linking forcing data, restarting the model, post-processing output data etc. The ESM-Tools have been developed by the Helmholtz ESM project. They are publicly available and make it easier for new OpenIFS users to get started with atmosphere-only and coupled simulations.

The OpenIFS developments at AWI and GEOMAR started with OpenIFS 40r1 in late 2017, and both institutes are now integrating OpenIFS 43r3 into their respective coupled models. The second release of OpenIFS 43r3 from ECMWF will include coupling interfaces to the sea ice–ocean models FESOM2 and NEMO/AGRIF. This will enable other licensed OpenIFS users to benefit from the developments at AWI and GEOMAR. Examples include the ongoing development of EC-Earth version 4 as well as new coupled climate models using OpenIFS in Italy and China. The joint development of the OpenIFS model for coupled climate modelling has also led to closer scientific collaboration between AWI, GEOMAR, the OpenIFS support team at ECMWF and the EC-Earth community as well as participation from all partners at the annual OpenIFS workshop and visits to ECMWF.

Model frameworks and early results

GEOMAR has set up configurations of FOCI2 with OpenIFS at low or high horizontal resolution for the atmosphere, coupled to NEMO with optional grid refinement with AGRIF. In the near future, FOCI2 will include coupling between NEMO and ECMWF's

	ECMWF-IFS climate configuration (PRIMAVERA project)	EC-Earth v3	CNRM-CM6	FOCI2 (OpenIFS)	AWI-CM3.1	EC-Earth v4
Atm	IFS Cycle 43r1	Based on IFS Cycle 36r4	ARPEGE-Climat v6	OpenIFS 43r3	OpenIFS 43r3	OpenIFS 43r3
Ocean	NEMO v3.4	NEMO v3.6	NEMO v3.6	NEMO v3.6	FESOM2	NEMO v4
Coupler	Single executable	OASIS3-MCT3	OASIS3-MCT3	OASIS3-MCT4	OASIS3-MCT4	OASIS3-MCT4
Horizontal res. Atm/Ocean	1° / 1° 0.25° / 0.25°	0.7° / 1° 0.35° / 0.25°	1.4° / 1°	1.1° / 0.5° 0.23° / [0.5°, 0.1°]	0.56° / [1°, 0.2°] 0.28° / [0.6°, 0.1°]	TBD
Grid refinement	No	No	No	AGRIF	Unstructured grid	No
Scope (realised/ planned)	AOGCM/AOGCM	ESM/ESM	AOGCM/ AOGCM	AOGCM/AOGCM	AOGCM/ESM	AOGCM/ESM

TABLE 1 Overview of the use of versions of the IFS, OpenIFS and the closely related ARPEGE model from Météo-France in current climate models. The scope denotes whether the model is/will be an Atmosphere–Ocean General Circulation Model (AOGCM) or a full Earth System Model (also including a biogeochemical model, dynamic vegetation and atmospheric chemistry). The ECMWF-IFS climate configuration is essentially an AOGCM but without river routing.

ECWAM ocean wave model and it will couple OpenIFS to the HD river routing scheme developed by Helmholtz Centre Geesthacht. AWI has developed AWI-CM3.1, which comprises OpenIFS at low or high horizontal resolution for the atmosphere, coupled to FESOM2 with the COREII (100–20 km) or HR (60–10 km) unstructured meshes (see Table 1). Long-term perspectives include ice-sheet and atmosphere–wave–ocean coupling with the PISM ice-sheet model and the MASNUM ocean wave model, respectively. Future developments of AWI-CM3.1 will be closely synchronised with EC-Earth version 4 and will therefore have ESM capabilities.

Atmospheric models forced with high-resolution sea-surface temperature data show a band of convergent surface winds and precipitation over the Gulf Stream. At the same time, climate models with a high-resolution ocean show that increasing the atmospheric resolution results in stronger eddy potential energy dissipation leading to stronger western boundary currents. This suggests that oceanic mesoscale eddy activity strongly influences atmospheric motions locally through air–sea fluxes of momentum, heat and freshwater. However, in most climate models the air–sea fluxes are calculated in the atmospheric model. This means that both the atmosphere and the ocean must have sufficiently high horizontal resolution for the oceanic mesoscale to influence the atmosphere. Hence, using an eddy-resolving ocean model of ~0.1° resolution coupled to a coarse-resolution atmosphere of ~2° resolution improves ocean dynamics and reduces surface biases, but the impact on the atmosphere will likely be underestimated.

Figure 2 demonstrates the capabilities of FOCI2 and AWI-CM3.1 by showing results from five years of simulation. Both models have comparable high-resolution atmosphere and ocean grids. The FOCI2 simulation has a 0.23° atmospheric resolution with a 0.5° ocean resolution with a grid refinement down to 0.1° in the North Atlantic. AWI-CM3.1 has a 0.28° atmospheric resolution with an unstructured ocean grid where horizontal resolution varies between 10 and 60 km and is finest where sea-surface height variance is largest. We have calculated the mean wintertime surface kinetic energy using daily output from AWI-CM3.1 and five-daily output from FOCI2. Both models exhibit an eddy-rich and energetic Gulf Stream and North Atlantic Current, indicating that the oceanic horizontal resolution is sufficient to resolve the baroclinic instabilities and eddy-mean flow interactions in the region. The Gulf Stream detaches slightly further north in FOCI2 compared to AWI-CM3.1. This could be the result of a coarser effective resolution in FOCI2. In the atmosphere, both models show a band of high precipitation anchored over the Gulf Stream, which is a clear signal that the oceanic mesoscale activity is felt by the atmosphere. Both AWI and GEOMAR are currently extending these simulations to span up to a century. They are also carrying out experiments using a low-resolution atmosphere to evaluate the impact of the high-resolution atmosphere on mean state and climate variability in climate models.

Benefits for weather forecasting

The results from climate modelling using OpenIFS can provide insights that will help ECMWF to evaluate the representation of coupled Earth system processes in the IFS and identify model biases. An accurate representation of such processes is particularly important at medium-range to seasonal timescales. With increasing lead time, weather forecasts tend towards the model climate, which should therefore be as realistic as possible. The asymptotic behaviour of the coupled model is also important for the development of coupled approaches to data assimilation and reanalysis. The results obtained when coupling the atmospheric and land components of the IFS to NEMO using grid-refinement or a different ocean model entirely (FESOM2) will also usefully complement the insights gained from the IFS climate configuration experiments carried out in the PRIMAVERA project.

Outlook

The OpenIFS model already is and will continue to be an important component for climate modelling at AWI and GEOMAR. Both institutes plan to use their respective high-resolution climate models for various projects for years to come. The ability to run climate models efficiently at high resolution, the world-leading science in the IFS, and the integration of active atmospheric chemistry and parallel netCDF I/O (XIOS) make the OpenIFS a very attractive atmospheric model for climate modelling projects. Ongoing and future projects with FOCI2 include the following:

- studying the role of the oceanic mesoscale in driving atmospheric extreme events (the ROADMAP project, funded by JPI Oceans)
- heat uptake over the Southern Ocean (SO-CHIC, an EU-funded Horizon 2020 project)
- the impact of Greenland meltwater on North Atlantic climate (G-shocx, funded by the German Research Foundation).

GEOMAR also plans to make coupled experiments with a global 0.25° ocean mesh and 0.05° refinement in the North Atlantic – an unprecedented resolution in coupled climate models. AWI-CM3.1 is earmarked for use in the second phase of the PalMod project (funded by the German Federal Ministry of Education and Research), which aims to study transient changes between glacial cycles. It will also be integrated into the Parallel Data Assimilation Framework (PDAF) developed at AWI. In addition, AWI has used OpenIFS to conduct atmosphere-only simulations for the World Climate

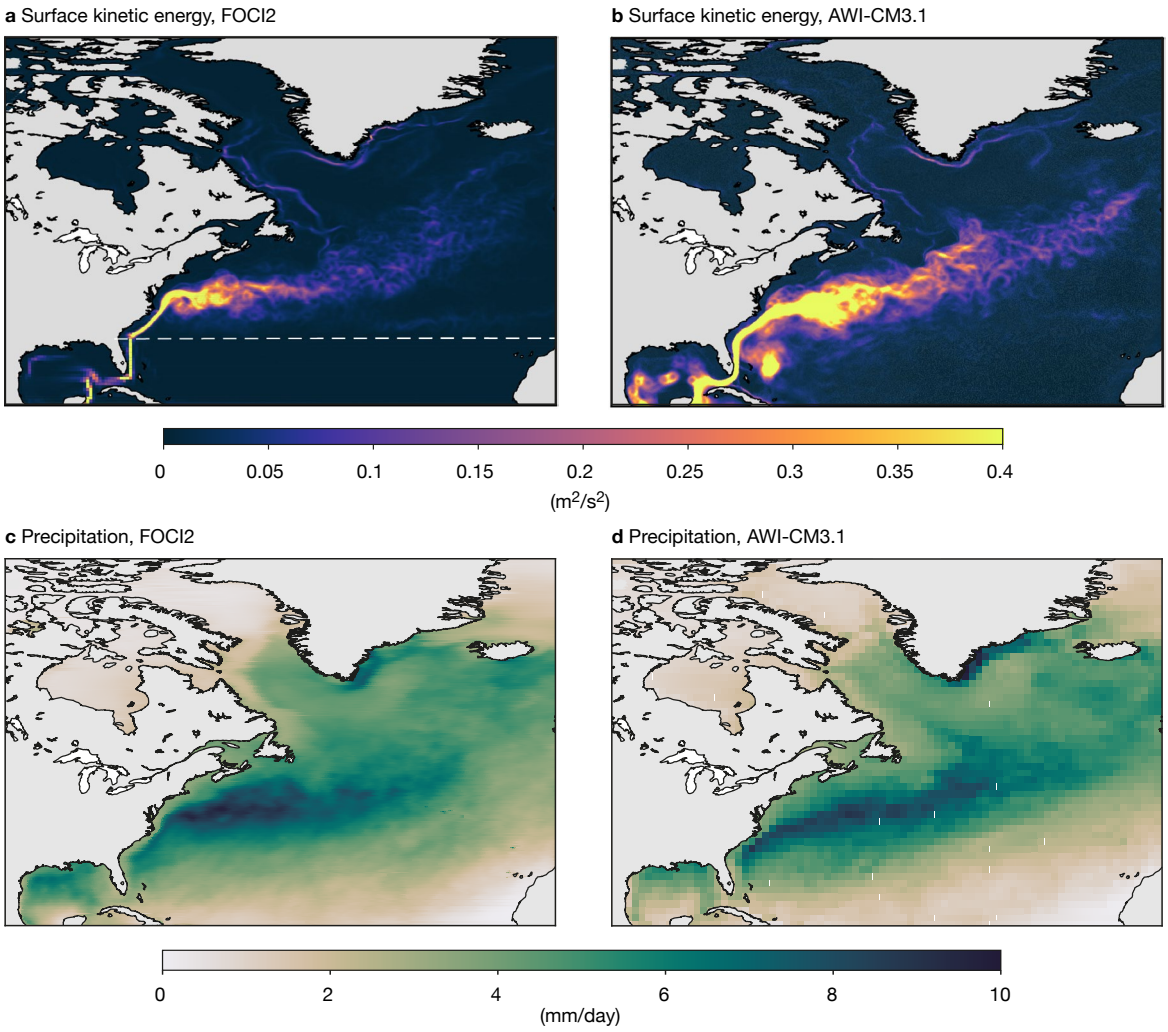

FIGURE 2 The charts show mean December–January–February values for (a) surface kinetic energy from FOCI2, (b) surface kinetic energy from AWI-CM3.1, (c) precipitation from FOCI2 and (d) precipitation from AWI-CM3.1. Kinetic energy is calculated from daily means in AWI-CM3.1 and five-daily means in FOCI. For FOCI2, the grid refinement is north of the white dashed line. Note that the resolution is 0.28° in AWI-CM3.1 but the output is coarse-grained to 1° resolution.

Research Programme's Polar Amplification Model Intercomparison Project (PAMIP).

Integrating OpenIFS into the existing modelling systems at GEOMAR and AWI has made it possible to break new scientific ground by allowing the use of a variable-resolution ocean mesh coupled to a high-resolution atmosphere. It has also led to new fruitful collaborations between AWI, GEOMAR, ECMWF and the EC-Earth consortium. ECMWF stands to benefit from those collaborations as the results of climate modelling using OpenIFS can provide useful pointers for model development at ECMWF.

The integration of OpenIFS into ESM-Tools makes it easier for new OpenIFS users to get started. Using OpenIFS in FOCI2 and AWI-CM3.1 would not have been possible without the support of the OpenIFS team at ECMWF and the EC-Earth team, and we look forward to more collaborations with the growing OpenIFS community in the future.

Further reading

Barbi, **D.**, **N. Wieters**, **P. Gierz**, **F. Chegini**, **S. Khosravi** & **L. Cristini**, 2020: ESM-Tools Version 4.0: A modular infrastructure for stand-alone and coupled Earth System Modelling (ESM). *Submitted to Geoscientific Model Development*.

Matthes, **K.**, **A. Biastoch**, **S. Wahl**, **J. Harlaß**, **T. Martin**, **T. Brücher et al.**, 2020: The Flexible Ocean and Climate Infrastructure Version 1 (FOCI1): Mean State and Variability, *Geosci. Model Dev.*, **13**, 2533–2568, doi:10.5194/gmd-13-2533-2020.

Roberts, **C.D.**, **S. Keeley**, **F. Molteni**, **R. Senan**, & **Torben Königk**, 2018: Coordinated climate simulations using the IFS, *ECMWF Newsletter* **No. 157**, 6–7.

Sidorenko, **D.**, **T. Rackow**, **T. Jung**, **T. Semmler**, **D. Barbi**, **S. Danilov et al.**, 2015: Towards multi-resolution global climate modelling with ECHAM6-FESOM. Part 1: model formulation and mean climate. *Clim. Dyn.*, **44**, doi:10.1007/s00382-014-2290-6.

ECMWF publications

(see *www.ecmwf.int/en/research/publications*)

Technical Memoranda

867 **Mason**, **D.**, **J. Garcia-Pintado**, **H.L. Cloke**, **S. Dance** & **J. Munoz-Sabater**: Assimilating high resolution remotely sensed soil moisture into a distributed hydrologic model to improve runoff prediction. *June 2020*

866 **Sandu**, **I.**, **P. Bechtold**, **L. Nuijens**, **A. Beljaar** & **A. Brown**: On the causes of systematic forecast biases in near-surface wind direction over the oceans. *June 2020*

865 **Ben-Bouallegue**, **Z.**: Accounting for representativeness in the verification of ensemble forecasts. *June 2020*

864 **Rennie**, **M.** & **L. Isaksen**: The NWP impact of Aeolus Level-2B Winds at ECMWF. *June 2020*

863 **Geer**, **A.J.**: Learning earth system models from observations: machine learning or data assimilation? *May 2020*

ESA Contract Reports

de Rosnay, **P.** & **P. Weston**: SMOS Operational Emergency Services CCN1: SMOS long term assessment based on re-analyses: strategy and work plan. *December 2019*

Baugh, **C.**, **P. de Rosnay** & **H. Lawrence**: SMOS Operational Emergency Services – Floods. *August 2019*

Lawrence, **H.**, **P. de Rosnay** & **C. Baugh**: ECMWF report: First steps towards using SMOS soil moisture in the European Flood Awareness System. *June 2019*

de Rosnay, **P.**, **J. Muñoz-Sabater**, **C. Albergel**, **H. Lawrence**, **L. Isaksen** & **S. English**: ECMWF Final Report on SMOS brightness temperature activities over land: Monitoring and Data Assimilation. *March 2019*

EUMETSAT/ECMWF Fellowship Programme Research Reports

54 **Lean**, **K.** & **N. Bormann**: Replacement of GOES-15 with GOES-17 AMVs. *May 2020*

53 **Lonitz**, **K.** & **A.J. Geer**: Reducing the drying effect through a water vapour correction to the all-sky error model. *May 2020*

ECMWF Calendar 2020/21

Sep 14–18	Annual Seminar: Numerical methods for atmospheric and oceanic modelling – recent advances and future prospects
Sep 15	Council (extraordinary session)
Oct 5–8	ECMWF–ESA workshop on machine learning for Earth observation and prediction
Oct 5–8	Training course: Use and interpretation of ECMWF products
Oct 12–14	Scientific Advisory Committee
Oct 14	Advisory Committee of Co-operating States
Oct 15–16	Technical Advisory Committee
Oct 19–20	Finance Committee
Oct 20	Policy Advisory Committee
Nov 2–5	ECMWF/EUMETSAT NWP SAF workshop on the treatment of random and systematic errors in satellite data assimilation for NWP
Dec 8–9	Council

Feb 1–4	Training course: Use and interpretation of ECMWF products
Mar 15–19	Training course: Parametrization of subgrid physical processes
Mar 22–26	Training course: Predictability and ensemble forecast systems
Apr 12–16	Advisory Committee for Data Policy and data policy meetings of EUMETSAT and ECOMET
Apr 19–23	Training course: Advanced numerical methods for Earth system modelling
Apr 27–28	Finance Committee
Apr 28	Policy Advisory Committee
May 4–7	Training course: EUMETSAT/ECMWF NWP SAF satellite data assimilation
May 10–14	Training course: Data assimilation
May 17–20	International workshop on ocean data assimilation methods
May 17–21	Online computing training week
Jun 1–4	Using ECMWF's Forecasts (UEF2021)

Contact information

ECMWF, Shinfield Park, Reading, RG2 9AX, UK

Telephone National 0118 949 9000

Telephone International +44 118 949 9000

Fax +44 118 986 9450

ECMWF's public website *www.ecmwf.int/*

E-mail: The e-mail address of an individual at the Centre is firstinitial.lastname@ecmwf.int. For double-barrelled names use a hyphen (e.g. j-n.name-name@ecmwf.int).

For any query, issue or feedback, please contact ECMWF's Service Desk at *servicedesk@ecmwf.int*.

Please specify whether your query is related to forecast products, computing and archiving services, the installation of a software package, access to ECMWF data, or any other issue. The more precise you are, the more quickly we will be able to deal with your query.

ECMWF

Newsletter | **No. 164** | Summer 2020

European Centre for Medium-Range Weather Forecasts

www.ecmwf.int